INFECTION AND IMMUNITY, May 2009, p. 1757–1773 Vol. 77, No. 5
0019-9567/09/$08.00+0 doi:10.1128/IAI.01485-08

Francisella tularensis Phagosomal Escape Does Not Require Acidification of the Phagosome[▽]

Daniel L. Clemens,* Bai-Yu Lee, and Marcus A. Horwitz

Division of Infectious Diseases, Department of Medicine, University of California-Los Angeles School of Medicine, Center for Health Sciences, Los Angeles, California 90095-1688

Received 4 December 2008/Returned for modification 11 January 2009/Accepted 9 February 2009

Following uptake, *Francisella tularensis* enters a phagosome that acquires limited amounts of lysosome-associated membrane glycoproteins and does not acquire cathepsin D or markers of secondary lysosomes. With additional time after uptake, *F. tularensis* disrupts its phagosomal membrane and escapes into the cytoplasm. To assess the role of phagosome acidification in phagosome escape, we followed acidification using the vital stain LysoTracker red and acquisition of the proton vacuolar ATPase (vATPase) using immunofluorescence within the first 3 h after uptake of live or killed *F. tularensis* subsp. *holarctica* live vaccine strain (LVS) by human macrophages. Whereas 90% of the phagosomes containing killed LVS stained intensely for the vATPase and were acidified, only 20 to 30% of phagosomes containing live LVS stained intensely for the vATPase and were acidified. To determine whether transient acidification might be required for phagosome escape, we assessed the impact on phagosome permeabilization of the proton pump inhibitor bafilomycin A. Using electron microscopy and an adenylate cyclase reporter system, we found that bafilomycin A did not prevent phagosomal permeabilization by *F. tularensis* LVS or virulent type A strains (*F. tularensis* subsp. *tularensis* strain Schu S4 and a recent clinical isolate) or by "*F. tularensis* subsp. *novicida*," indicating that *F. tularensis* disrupts its phagosomal membrane by a mechanism that does not require acidification.

Francisella tularensis is a gram-negative facultative intracellular bacterium that causes a zoonosis in animals and a potentially fatal infection, tularemia, in humans. *F. tularensis* consists of four subspecies, *F. tularensis* subsp. *tularensis*, *F. tularensis* subsp. *holarctica*, *F. tularensis* subsp. *mediasiatica* and "*F. tularensis* subsp. *novicida*," whose geographic distributions and virulence in humans differ (12, 25). *F. tularensis* subsp. *tularensis* (type A), found almost exclusively in North America, is highly virulent for humans. As few as 10 organisms received subcutaneously or 25 organisms received by inhalation can lead to a severe infection (32, 33). *F. tularensis* subsp. *holarctica* (type B, found in North America and in Europe) and *F. tularensis* subsp. *mediasiatica* (found in Asia) are less virulent. *F. tularensis* subsp. *novicida*, found in North America and Australia, is virulent in mice and has occasionally been reported to cause a mild disease, compared with type A infections, in humans (38). Because of its high infectivity and capacity to cause severe morbidity and mortality, *F. tularensis* subsp. *tularensis* is considered a potential agent of bioterrorism and is classified as a category A select agent.

In animal models of tularemia, macrophages are important host cells for *F. tularensis*, and the virulence of the bacterium correlates with its capacity to grow in macrophages (2, 20). We have shown previously that efficient uptake of *F. tularensis* subsp. *tularensis* and *F. tularensis* subsp. *holarctica* live vaccine strain (LVS) by human macrophages requires complement and that it is mediated by a unique process involving spacious, asymmetric pseudopod loops (10). The mannose receptor (34) and class A scavenger receptors (26) have also been reported to play a role in uptake of *F. tularensis* LVS. We have demonstrated that following uptake, the bacterium enters a membrane-bound vacuole that acquires limited amounts of endosomal markers, including limited amounts of the late endosomal-lysosomal markers CD63, LAMP1, and LAMP2, but that the vacuole does not acquire the acid hydrolase cathepsin D, does not fuse with lysosomes, and is only minimally acidified to a pH of 6.7 at 3 h postinfection (11). With additional time after uptake, *F. tularensis* disrupts the phagosomal membrane and the bacterium escapes and replicates in the host cell cytosol (9, 11, 16). Celli and coworkers have studied the interaction of mouse bone marrow-derived macrophages with *F. tularensis* LVS (6) and *F. tularensis* Schu S4 (7) and also reported a transient interaction with the host endocytic pathway prior to escape with a more rapid kinetic profile than we have observed in human monocyte-derived macrophages (MDM). In addition, Chercoun et al. (6) have reported that at late times after infection (20 h) in mouse macrophages, a large proportion of *F. tularensis* cells enter an autophagosomal compartment. The *Francisella* pathogenicity island has been shown to be essential for the altered intracellular trafficking and escape of *F. tularensis* subsp. *holarctica* LVS (22) and *F. tularensis* subsp. *novicida* (31) into the cytoplasm.

Some degree of acidification has been shown to be required for the escape of certain intracellular pathogens that replicate in the cytosol. For example, acidification of the vacuole occupied by *Listeria monocytogenes* is required for activation of listeriolysin O for permeablization of the vacuole (1), and acidification of either early or late endosomes is required for pH-dependent changes in adenoviral proteins to mediate the translocation of adenovirus into the host cell cytoplasm (23). While we have reported previously that the *F. tularensis* phago-

* Corresponding author. Mailing address: Division of Infectious Diseases, Department of Medicine, UCLA School of Medicine, CHS 37-121, 10833 LeConte Avenue, Los Angeles, CA 90095-1688. Phone: (310) 825-9324. Fax: (310) 794-7156. E-mail: dclemens@mednet.ucla.edu.

▽ Published ahead of print on 23 February 2009.

some is only minimally acidified to a pH of 6.7 at 3 h postinfection, this finding does not preclude the possibility that some degree of acidification, even transient acidification, might be required for the bacterium to disrupt its phagosome and escape into the cytoplasm. Indeed, Santic et al. recently reported that nearly 80 to 85% of *F. tularensis* subsp. *novicida* phagosomes are acidified at 15 to 30 min postinfection in human MDM and that inhibition of acidification with bafilomycin A completely blocks escape (30). In contrast to these results for human macrophages with *F. tularensis* subsp. *novicida*, Chong et al. (7) have recently reported that *F. tularensis* Schu S4 phagosomes in mouse bone marrow-derived macrophages are transiently acidified and that inhibition of acidification delays, but does not prevent, phagosome disruption. To explore the importance of phagosomal pH on subsequent intracellular trafficking events for *F. tularensis* in human macrophages, we have examined the time course of colocalization of *F. tularensis* with the proton vacuolar ATPase (vATPase) and with a vital stain for acidified compartments, and we have examined the effect of inhibitors of acidification on phagosomal disruption.

MATERIALS AND METHODS

Bacterial strains and growth conditions. *F. tularensis* subsp. *tularensis* strain Schu S4, a virulent recent clinical isolate (RCI) of *F. tularensis* subsp. *tularensis* (type A) (NY 96-3369), and *F. tularensis* subsp. *holarctica* LVS were obtained from the Centers for Disease Control and Prevention, Atlanta, GA. IglC-null LVS (ΔiglC-LVS) was obtained from Anders Sjostedt, Umea, Sweden (22). *F. novicida* strain U112 was obtained from Karl Klose, San Antonio, TX. The bacteria were passaged through monolayers of macrophage-like THP-1 cells to ensure virulence and stored frozen at −85°C. Before each infection experiment, the bacteria were thawed, grown for 1 to 2 days on chocolate agar plates enriched with IsoVitaleX and hemoglobin, suspended in normal saline, and diluted with RPMI 1640 medium containing fresh 10% autologous or AB serum to obtain the desired multiplicity of infection (MOI). Killed *F. tularensis* LVS was prepared by treatment of the bacteria with 4% paraformaldehyde for 30 min at room temperature, removal of the fixative by centrifugation at 17,000 × *g* for 15 min, resuspension, and washing in phosphate-buffered saline (PBS) three times. Bacterial aggregates generated by the fixation and centrifugation process were removed by low-speed centrifugation at 200 × *g* for 10 min prior to use of the bacteria in an infection experiment.

Preparation of LVS-GFP. To prepare LVS-GFP, the pFNLTP plasmid containing a β-lactamase gene (*bla*), a neomycin phosphotransferase gene (*npt*) conferring kanamycin resistance, a pUC replication origin, and a gene encoding green fluorescence protein (GFP) under the control of the *F. tularensis groE* promoter, generously provided by Thomas Zahrt (Medical College of Wisconsin), was electroporated into LVS. LVS transformants were selected by growth on chocolate agar containing kanamycin, and GFP expression was verified by Western immunoblotting and by fluorescence microscopy.

Human serum, cells, and cell line. Human serum was prepared and handled in a manner that preserved complement activity (18). Heat-inactivated serum was prepared by incubation of the serum at 56°C for 30 min.

Peripheral blood mononuclear cells were isolated (11), the concentration was adjusted to 3×10^6 cells/ml in RPMI 1640 medium with glutamine (Mediatech, Manassas, VA) and 20% autologous serum, and the cells were incubated for 5 days in sterile screw-cap Teflon wells (Savillex Corp. Minnetonka, MN) at 37°C in the presence of 5% CO_2. Teflon wells were chilled on ice, and the MDM were resuspended, washed, and allowed to adhere to plastic tissue culture plates or glass coverslips for 1 day prior to use in infection experiments (11). The UCLA Institutional Review Board approved the participation of normal human blood donors in our research.

The human monocytic cell line THP-1 (ATCC TIB 202), was grown in RPMI 1640 medium supplemented with 2 mM glutamine and 10% heat-inactivated fetal bovine serum. Prior to use in an infection experiment, the THP-1 cells were added (1.5×10^5 cells/cm^2) to glass coverslips in 2-cm^2 tissue culture wells or to plastic tissue culture plates and differentiated with phorbol 12-myristate 13-acetate (PMA) (100 nM) in RPMI 1640 medium with 10% heat-inactivated fetal bovine serum for 3 days at 37°C in air containing 5% CO_2.

Analysis of phagosome escape by electron microscopy. Prior to infection with *F. tularensis*, macrophage monolayers (either MDM or THP-1 cells) were left untreated or were pretreated for 30 min with inhibitors of acidification at the following concentrations: 20 mM ammonium chloride, 40 μM chloroquine, and 250 nM bafilomycin. Because inhibition of endosomal acidification prevents the release of iron from iron-transferrin and causes iron deprivation and suppression of intracellular growth of *F. tularensis* (13), we supplemented culture media containing acidification inhibitors with ferric ammonium citrate at a concentration of 0.1 mg/ml (17.5 μg/ml of iron). We have previously demonstrated that supplementation of culture medium with this level of iron chelate overcomes the iron deprivation related to inhibition of endosomal acidification (3, 4). Alternatively, we supplemented the culture medium with ferric pyrophosphate (50 μg/ml [6 μg/ml of iron]), a level found by Fortier et al. (13) to restore nearly complete intracellular growth of *F. tularensis* LVS in the presence of 20 mM NH_4Cl. To synchronize uptake, we opsonized *F. tularensis* bacteria in 10% fresh human AB serum for 10 min at 37°C, centrifuged the bacteria onto macrophage monolayers at 1,000 × *g* for 30 min at 4°C (in culture medium with or without the same concentration of inhibitors and iron) at an MOI of 3:1 (ratio of bacteria to macrophages), and incubated the monolayers at 37°C for 20 min to allow uptake. The monolayers were washed, incubated for 3 to 7 h in culture medium with or without the same concentrations of inhibitors and ferric ammonium citrate, fixed, and processed for electron microscopy (11). Bacteria were scored as "free" in the cytoplasm if less than 50% of the bacterial circumference was surrounded by a membrane bilayer. In most cases, the distinctions were unequivocal; the "free" bacteria were totally free, and the "bound" bacteria were enclosed within easily discernible membrane bilayers. (Only 9% of the bacteria encountered were in an intermediate state, and most of these bacteria were either 90% free or 90% bound). Specimens were viewed and photographed with a JEOL 100 CX transmission electron microscope at 80 kV using Kodak electron microscope film, and the images scanned and assembled with Adobe Photoshop CS.

Analysis of phagosome escape using a reporter system for phagosome permeabilization. Adenylate cyclase catalyzes the conversion of ATP to cyclic AMP (cAMP) only in the presence of calmodulin, a cytosolic protein. Thus, a recombinant adenylate cyclase secreted by *F. tularensis* can be used to report the degree to which *F. tularensis* secreted proteins have access to calmodulin in the host cytosol. We have shown previously that catalase peroxidase (KatG) is released extracellularly by *F. tularensis* growing in liquid cultures and within macrophages (21). To prepare recombinant *F. tularensis* with the capacity to secrete adenylate cyclase, we constructed an in-frame fusion of the *F. tularensis katG* sequence corresponding to its leader peptide and the first 20 amino acids of mature KatG and *cyaA′*, a 1.2-kb DNA fragment encoding the amino-terminal adenylate cyclase domain of the *Bordetella pertussis* cyclolysin (CyaA) from pMJW1753 (provided by Kaoru Geddes [15]), and placed it under the control of the *F. tularensis groE* promoter in pFNLTP. The plasmid was electroporated into LVS or the *iglC*-deficient mutant of LVS (ΔiglC-LVS, kindly provided by Anders Sjostedt), and recombinant bacteria (LVS-sCyaA′ and ΔiglC-LVS-sCyaA′) were selected by growth on chocolate agar with kanamycin. As a control, we also prepared recombinant LVS and ΔiglC-LVS expressing a nonsecreted form of CyaA′ lacking the KatG leader sequence. We verified by Western immunoblotting using monoclonal antibody 3D1 (diluted 1:750) directed against adenylate cyclase (Santa Cruz Biotechnology Inc.) that LVS-CyaA′ and LVS-sCyaA′ express comparable amounts of the CyaA′ protein but that only LVS-sCyaA′ releases significant amounts of the recombinant protein into liquid culture medium. We used rabbit polyclonal antibodies directed against *F. tularensis* IglC (1:10,000 dilution) and bacterioferritin (1:10,000 dilution) as controls for loading of bacterial proteins. The Western immunoblots were stained with secondary antibodies (1:5,000 dilution of goat anti-mouse immunoglobulin G [IgG] peroxidase conjugate or 1:20,000 dilution of goat anti-rabbit peroxidase conjugate), developed with WestPico (Pierce) chemiluminescent substrate, and imaged with X-ray film (Kodak).

To assay for phagosome permeabilization, we infected monolayers of PMA-differentiated macrophage-like THP-1 cells (3×10^5 cells/well) in 24-well tissue culture plates with LVS-sCyaA′ (or, as a control, LVS-CyaA′) and at different times after infection washed the monolayers with PBS and added 0.1 N HCl to extract the cAMP. The extracted cAMP was neutralized with NaOH and measured by an enzyme-linked immunosorbent assay performed according to the manufacturer's instructions (Assay Designs, Ann Arbor, MI). Adenylate cyclase enzymatic activity was measured by measuring the conversion of [^{32}P]ATP to [^{32}P]cAMP using a modification of previously described procedures (27). Briefly, 10 μl of a bacterial culture filtrate was incubated at 30°C for 15 min in 100 μl of assay medium containing 30 mM HEPES (pH 7.5), 5 mM $MgCl_2$, 100 mM NaCl, 20 μM [α-^{32}P]ATP (10 μCi/ml), 1 μM calmodulin, 10 μM $CaCl_2$, 5 mM phosphocreatine, and 12.5 U/ml creatine phosphokinase (to regenerate ATP). The

reaction was terminated by addition of 100 μl of 2% sodium dodecyl sulfate containing 20 mM ATP and 1 mM unlabeled cAMP, the [^{32}P]cAMP formed was isolated by the Dowex 50W-X4 neutral alumina double-column method (29), and radioactivity was measured in Ecoscint XR with a Beckman LS6500 liquid scintillation counter.

Determination of numbers of bacterial CFU in macrophage monolayers. A synchronized infection of macrophage monolayers was established as described above, and gentamicin (0.1 μg/ml) was added to the culture medium after the initial infection to prevent growth of LVS in the culture medium. We have found that hypotonic lysis of macrophage monolayers by distilled water or by detergent does not lead to optimal recovery of bacterial CFU due to incomplete lysis of macrophages by distilled water and the impact of the detergent on bacterial viability. To determine the numbers of bacteria in macrophage monolayers, we washed the monolayers in culture medium containing 20 mM HEPES (pH 7.4) and scraped the cells with cell scrapers (Costar) into 1.5 ml of 0.25 M sucrose, 20 mM HEPES (pH 7.4). The suspension was transferred to a tube (1 cm by 10 cm) containing 20 3-mm glass beads and vortexed 10 times for 2 s. We found by using phase-contrast and fluorescence microscopy that this method consistently liberated more than 95% of bacteria from the macrophages and that vortexing the bacteria with glass beads in this medium did not decrease the number of CFU.

Assessment of the pH of *F. tularensis* compartments by LysoTracker red staining. Live or killed *F. tularensis* LVS-GFP and latex beads (diameter, 1 μm) were preopsonized by incubation for 10 min in 20% human AB serum at 37°C, the concentration was adjusted so that the MOI was 2:1 (ratio of bacteria to macrophages) for the bacteria and the latex beads (adjusted to a final concentration of 2.5×10^{-4}% solids), and the preparation was centrifuged onto monolayers of PMA-differentiated THP-1 cells or MDM on glass coverslips in 24-well plates at 4°C at 1,000 × *g* for 30 min. The monolayers were incubated at 37°C for 20 min and washed, the medium was replaced with fresh culture medium, and the monolayers were incubated for an additional 15 min to 6 h and fixed with 4% paraformaldehyde, 0.1 M piperazine-*N*,*N*′-bis(2-ethanesulfonic acid) (PIPES) (pH 7.4), 6% sucrose. LysoTracker red DND-99 was added to the culture medium at a concentration of 0.1 μM 15 min prior to fixation. After fixation, the monolayers were washed in 0.1 M PIPES (pH 7.4), 6% sucrose, and extracellular bacteria were stained by incubation first with 1:1,000 rabbit anti-*F. tularensis* IgG (Becton Dickinson) in the same buffer containing 0.1% bovine serum albumin and 5% goat serum and then with a 1:50 dilution of amino-methyl coumarin (AMCA)-conjugated goat anti-rabbit IgG. The monolayers were washed in PBS and mounted in Prolong antifade mounting medium (Molecular Probes), epifluorescence was examined with an Eclipse TE2000-S microscope equipped with an X-Cite 120 light source (Nikon), and images were acquired with a SPOT RT-KE monochrome camera and SPOT software (Diagnostic Instruments, Sterling Heights, MI). Images were assembled with Adobe Photoshop CS software.

To determine the impact of inhibitors of acidification on phagosomal pH, we examined the extent of colocalization of LysoTracker red DND-99 with paraformaldehyde-killed LVS-GFP in PMA-differentiated THP-1 cells or MDM with or without treatment with the inhibitors. Monolayers of MDM or PMA-differentiated THP-1 macrophages were left untreated or were pretreated for 30 min with ammonium chloride, chloroquine, or bafilomycin A, incubated for 60 min with killed GFP-expressing *F. tularensis* LVS in RPMI 1640 (with or without inhibitors) containing 10% AB serum, washed to remove extracellular bacteria, and incubated in culture medium with or without inhibitors of acidification for 3 h. LysoTracker red DND-99 was added to the monolayers 15 min prior to fixation, and the preparations were observed by using fluorescence microscopy as described above.

Immunofluorescence evaluation of the distribution of vATPase. THP-1 cells were allowed to ingest live or killed *F. tularensis* LVS-GFP and fluorescent blue latex beads and were fixed for immunofluorescence microscopy at different times following uptake, as described above for LysoTracker red staining, except that the monolayers were fixed in freshly prepared 4% paraformaldehyde in 0.075 M sodium phosphate (pH 7.4) for 30 min, washed twice with PBS, transferred to antigen retrieval buffer (5% [wt/vol] urea, 100 mM Tris-HCl; pH 9.5), and heated to 80 to 90°C for 15 min. The coverslips were washed with PBS and permeabilized by incubation in 0.1% saponin in PBS containing 10 mM glycine for 30 min, nonspecific antigenic sites were blocked by incubation in 5% goat serum in PBS containing 1% bovine serum albumin, and vATPase subunit 6A was stained with chicken polyclonal antibody (GenWay), followed by Texas Red-conjugated goat anti-chicken IgY antibody. Host nucleic acid was stained with 4′,6′-diamidino-2-phenylindole (DAPI), and the coverslips were mounted and viewed by epifluorescence microscopy as described above. Because the chicken polyclonal antibody was found to have some weak cross-reactivity with *F. tularensis* antigens, we preadsorbed the antibody against *F. tularensis* LVS acetone powder (17). Immunofluorescence verified that the resulting preadsorbed antibody had no cross-reactivity with *F. tularensis*.

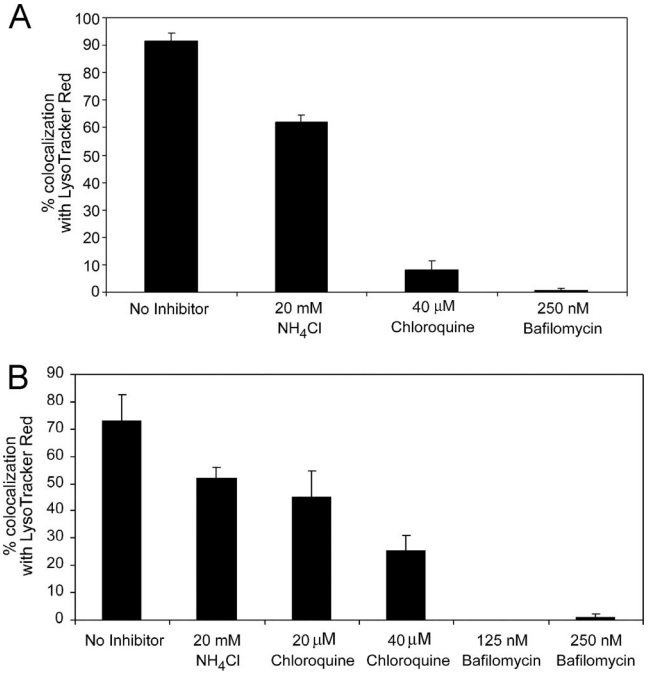

FIG. 1. Impact of NH_4Cl, chloroquine, and bafilomycin A on acidification of vacuoles occupied by killed *F. tularensis* in MDM (A) and THP-1 cells (B). To assess the capacity of NH_4Cl, chloroquine, and bafilomycin A to block acidification, we used fluorescence microscopy to determine the extent of colocalization of paraformaldehyde-killed GFP-expressing *F. tularensis* with LysoTracker red DND-99, a fluorescent dye that labels acidified compartments, at 3 h (A) and 8 h (B) postinfection. Ammonium chloride, chloroquine, and bafilomycin A all caused a marked decrease in colocalization of killed *F. tularensis* with LysoTracker red in MDM (A) and in THP-1 cells (B). The bars and error bars indicate the means and standard deviations of duplicate determinations for at least 40 bacteria.

RESULTS

Impact of acidification inhibitors: assessment by transmission electron microscopy. We have shown previously by ultrastructural analysis of both infected human MDM and infected THP-1 monocyte-like cells that *F. tularensis* disrupts its phagosome and escapes into the host cell cytoplasm (11). We have demonstrated similar kinetics of escape both for the attenuated LVS strain and for a virulent recent clinical isolate (RCI) of the type A strain; approximately 15% of *F. tularensis* was free in the cytoplasm at 3 h postinfection, and 35 to 50% was free in the cytoplasm by 5 to 7 h postinfection (11). Here, using fluorescence microscopy, we first studied the impact of three commonly used inhibitors of acidification, ammonium chloride, chloroquine, and bafilomycin A, on colocalization of LysoTracker red (a fluorescent dye that labels acidified compartments) with phagosomes containing GFP-expressing paraformaldehyde-killed *F. tularensis* LVS (which resides in acidified phagolysosomes [11]). We found that bafilomycin A (an agent that disrupts the vacuolar proton pump) completely abolished LysoTracker red staining of MDM at 3 h after uptake (Fig. 1A). As expected, the lysosomotropic agents ammonium chloride and chloro-

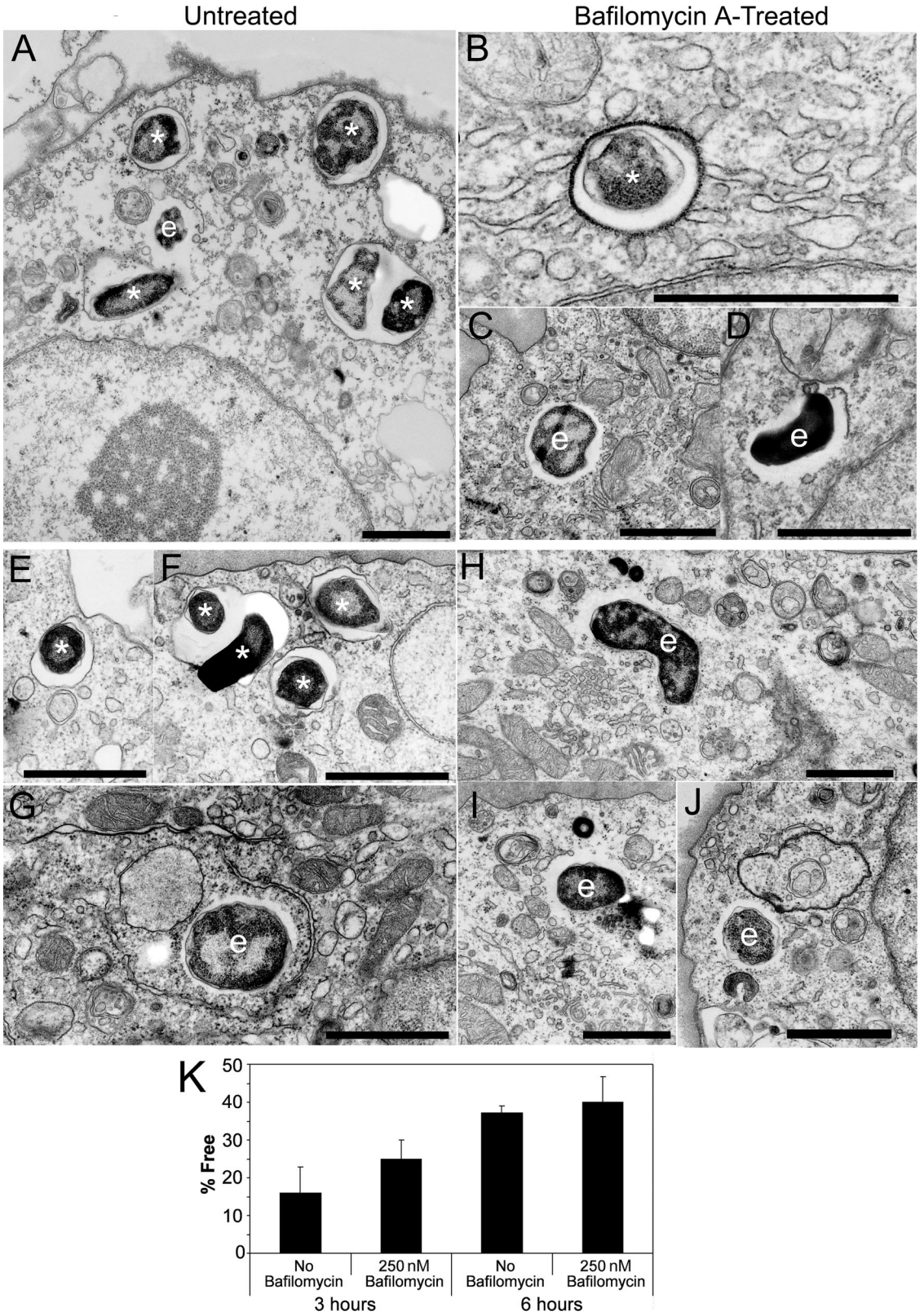

FIG. 2. Ultrastructural analysis of the impact of bafilomycin A on *F. tularensis* Schu S4 phagosome escape in human THP-1 macrophage-like cells. THP-1 macrophage-like cells were left untreated (A and E to G) or were pretreated for 30 min with bafilomycin A (B to D and H to J) prior to infection with *F. tularensis* Schu S4 in the presence or absence of 250 nM bafilomycin A and 0.1 mg/ml ferric ammonium citrate. Infection was continued for 3 h (A to D) or 6 h (E to J) under the same conditions prior to fixation and preparation of the monolayers for transmission electron microscopy. *F. tularensis* Schu S4 bacteria residing within vacuoles with clearly defined membrane bilayers in untreated macrophages at 3 h (A) and

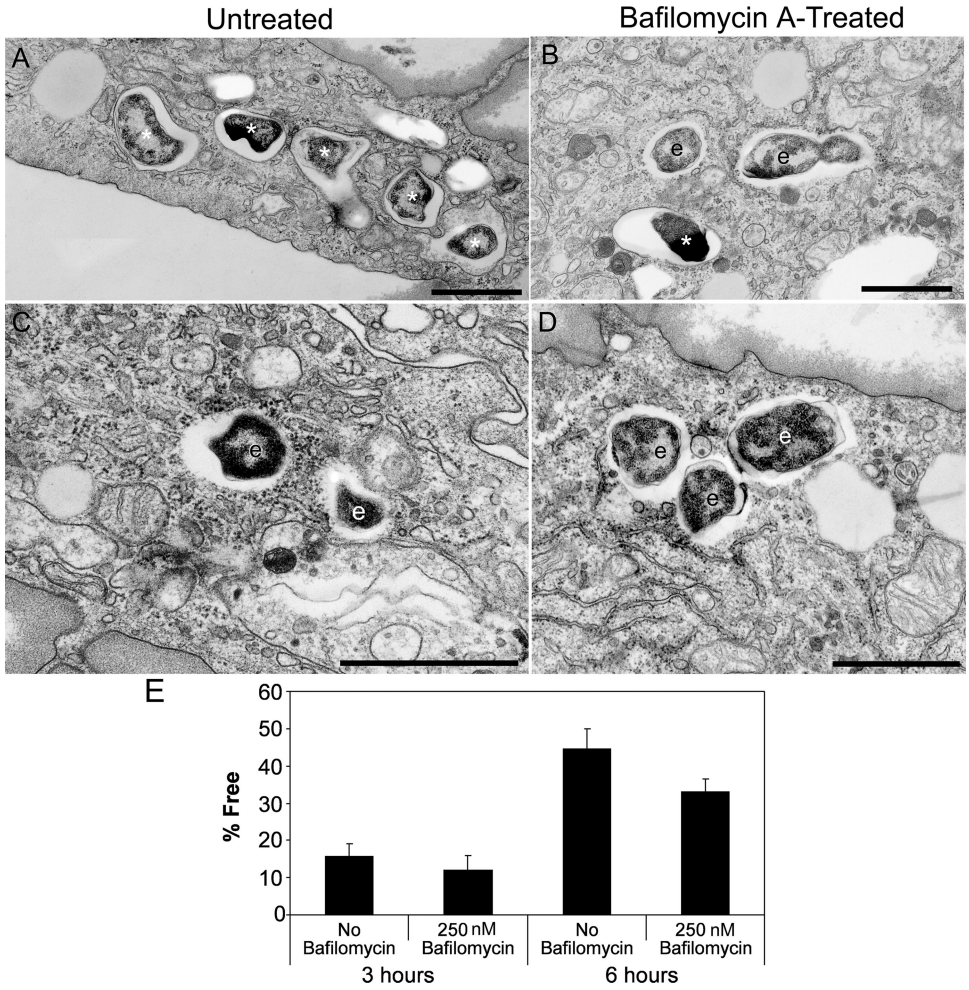

FIG. 3. Ultrastructural analysis of the impact of bafilomycin A on *F. tularensis* Schu S4 phagosome escape in human MDM. Monolayers of human MDM were left untreated (A and C) or were pretreated for 30 min with bafilomycin A (B and D) prior to infection with *F. tularensis* Schu S4 in the presence or absence of 250 nM bafilomycin A and 0.1 mg/ml ferric ammonium citrate as described in the legend to Fig. 1. Infection was continued for 3 h (A and B) or 6 h (C and D) under the same conditions prior to fixation and preparation of the monolayers for transmission electron microscopy. *F. tularensis* Schu S4 bacteria residing within vacuoles with easily discernible membrane bilayers are indicated by asterisks (A and B), and bacteria that escaped into the cytoplasm are indicated by "e" (B, C, and D). Size bars = 0.5 μm. (E) Percentages of *F. tularensis* Schu S4 bacteria that escaped into the cytoplasm. Treatment of the MDM with bafilomycin A did not prevent escape of *F. tularensis* Schu S4 into the cytoplasm. The bars and error bars indicate the means and standard errors for assessments of at least 40 cells on each of three electron microscopy grids.

quine also decreased acidification of the killed *F. tularensis* phagolysosomal compartment, but the inhibition of acidification was less complete than that provided by bafilomycin A (Fig. 1A). We verified that these inhibitors have a similar impact on acidification in THP-1 cells and that the inhibition was still evident 8 h after uptake of the killed LVS-GFP (Fig. 1B).

To determine whether acidification of the phagosomal compartment is required for escape of *F. tularensis* into the cytoplasm, we treated human MDM or THP-1 cells with bafilomycin A for 30 min prior to infection and for 3 to 6 h after infection with *F. tularensis* and assessed phagosomal disruption by transmission electron microscopy. We observed that bafilomycin A treatment does not prevent escape of *F. tularensis* Schu S4 into the cytoplasm of THP-1 cells (Fig. 2) or MDM (Fig. 3). Similarly, we observed that bafilomycin A treatment of human MDM does not prevent escape into the cytoplasm of a virulent recent clinical isolate (RCI) of *F. tularensis* subsp. *tularensis* (Fig. 4), *F. tularensis* subsp. *holarctica* LVS (Fig. 5),

6 h (E to F) postinfection are indicated by asterisks. An *F. tularensis* Schu S4 bacterium at 3 h postinfection residing within a vacuole with a densely staining fibrillar coat in a bafilomycin A-treated macrophage is also indicated by an asterisk (B). *F. tularensis* Schu S4 bacteria that escaped into the cytoplasm in untreated macrophages at 3 h (A) or 6 h (G) or in macrophages treated with bafilomycin A at 3 h (C and D) or 6 h (H to J) are indicated by "e." Size bars = 0.5 μm. (K) Percentages of *F. tularensis* Schu S4 bacteria that escaped into the cytoplasm. In the absence or presence of bafilomycin A, 15 to 25% of *F. tularensis* Schu S4 bacteria escaped into the cytoplasm by 3 h and 40 to 45% escaped by 6 h. The bars and error bars indicate means and standard errors for assessments of at least 40 cells on each of three electron microscopy grids.

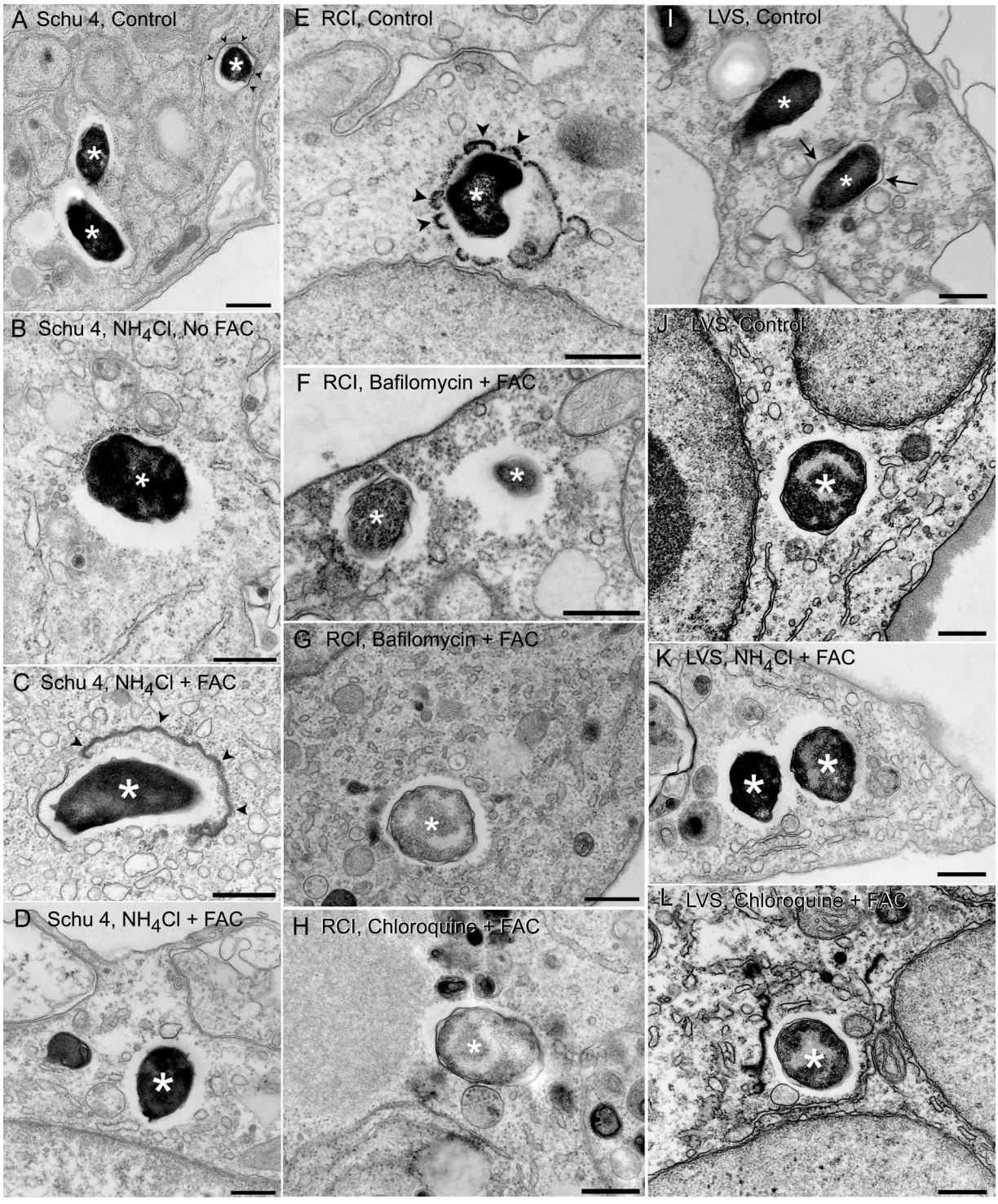
A Schu 4, Control
B Schu 4, NH4Cl, No FAC
C Schu 4, NH4Cl + FAC
D Schu 4, NH4Cl + FAC
E RCI, Control
F RCI, Bafilomycin + FAC
G RCI, Bafilomycin + FAC
H RCI, Chloroquine + FAC
I LVS, Control
J LVS, Control
K LVS, NH4Cl + FAC
L LVS, Chloroquine + FAC

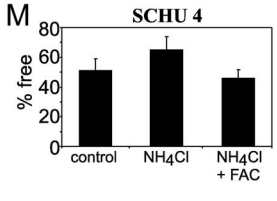
M
SCHU 4
% free
0
20
40
60
80
control
NH4Cl
NH4Cl + FAC

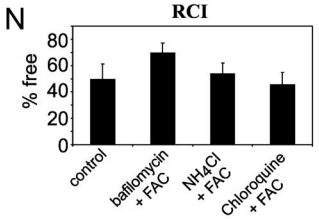
N
RCI
% free
0
20
40
60
80
control
bafilomycin + FAC
NH4Cl + FAC
Chloroquine + FAC

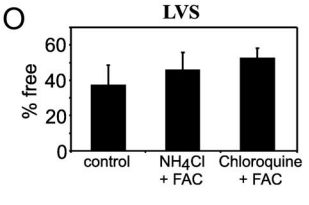
O
LVS
% free
0
20
40
60
control
NH4Cl + FAC
Chloroquine + FAC

or *F. tularensis* subsp. *novicida* (Fig. 6). We also observed that treatment of MDM with the lysosomotropic agent ammonium chloride does not prevent escape into the cytoplasm of Schu S4, RCI, or LVS and that treatment of MDM with the lysosomotropic agent chloroquine does not prevent escape into the cytoplasm of RCI or LVS, as assessed by transmission electron microscopy at 7 h postinfection (Fig. 4). The concentrations of the lysosomotropic agents ammonium chloride (20 mM) and chloroquine (40 μM) used in these studies were the concentrations shown previously to inhibit the intracellular growth of *F. tularensis* and *Legionella pneumophila* in macrophages (3, 13). In most cases, we added supplemental iron in order to ensure that we were examining a direct impact of inhibition of acidification rather than an indirect effect exerted through iron restriction. However, in the case of ammonium chloride, we observed no inhibition of escape of Schu S4 into the host cytoplasm with or without supplemental iron (Fig. 4).

Impact of inhibitors on growth. None of the inhibitors has any direct effect on growth of the bacteria in a chemically defined broth culture (Fig. 7A). We found that pretreatment of macrophages for 30 min with the acidification inhibitors (ammonium chloride, chloroquine, and bafilomycin A) consistently decreased uptake of the bacteria by the macrophages two- to threefold but that after uptake the bacteria were nevertheless able to multiply within the macrophages, resulting in an approximately 1-log increase over a 24-h period (Fig. 7B). The number of CFU in the culture supernatants was less than 10% of the number measured in the monolayers (data not shown). The inhibitors of acidification may alter membrane trafficking and receptor recycling rates within the macrophages, thereby altering the efficiency of uptake of the bacteria, as well as the subsequent growth of the bacteria, by mechanisms unrelated to phagosome permeabilization. In multiple experiments, we have observed that during the first 11 h after uptake, the rate of intracellular growth of bacteria in bafilomycin A-treated THP-1 cells is similar to that in untreated macrophages. However, over a longer period of time (e.g., 24 h, as shown in Fig. 7B), the overall rate of growth of LVS is significantly lower in bafilomycin A-treated macrophages than in untreated macrophages. Some decrease in the intracellular growth rate of the bacteria at later time points (e.g., 11 to 24 h) could be attributable to a variety of factors, including toxicity of the inhibitors to the macrophages, alterations in the minerals and nutrients available to the bacteria (due to alterations in macrophage metabolism), or decreased efficiency of phagosome permeabilization.

Impact of acidification inhibitors: assessment by a secreted adenylate cyclase reporter system. While we consider ultrastructural analysis to be the "gold standard" for assessing phagosomal disruption and escape into the cytoplasm of *F. tularensis*, we have also developed a biochemical method for assessing disruption of the phagosome to obtain independent confirmation of our findings. We introduced into *F. tularensis* a plasmid construct encoding either a nonsecreted adenylate cyclase (CyaA′) or a secreted form (sCyaA′) of the enzyme from *B. pertussis* by fusing the 1.2-kb *cyaA′* sequence to the leader sequence of *F. tularensis* KatG, an enzyme that we have shown is released extracellularly by *F. tularensis* growing either in liquid culture or in macrophages (21). We confirmed by Western immunoblotting and by measurement of enzymatic activity that adenylate cyclase was secreted into the culture filtrate of the LVS derivative encoding CyaA′ bearing the KatG leader sequence but not into the culture filtrate of the LVS derivative encoding CyaA′ without the leader sequence (Fig. 8). Adenylate cyclase generates cAMP from ATP only in the presence of the cytoplasmic protein calmodulin (39). Therefore, generation of cAMP by intracellular *F. tularensis* sCyaA′ occurs only if the phagosomal membrane has been permeabilized so that the secreted adenylate cyclase is in contact with host cell cytosolic calmodulin and ATP. Consistent with this, at 11 h postinfection, we detected markedly higher levels of cAMP generated in macrophages infected with LVS-sCyaA′ (which expresses a secreted form of CyaA′) than in monolayers infected with comparable numbers of LVS-CyaA′ (which expresses the nonsecreted form of CyaA′) or with greater numbers of *iglC*-null LVS-sCyaA′ (which expresses the secreted form of CyaA′ but is unable to escape into the cytoplasm) (Fig. 9A and B). Because the amount of adenylate cyclase released is influenced by the number of bacteria, we calculated the amount of cAMP generated per CFU and per each monolayer for each condition (Fig. 9C). Lower levels of cAMP per bacterium were detected in the LVS-sCyaA′-infected monolayers at 5 h postinfection than at 11 h postinfection (Fig. 9C), most

FIG. 4. Ultrastructural analysis of the impact of inhibitors of acidification on phagosome escape. Human MDM were left untreated (A, E, I, and J) (Control) or were pretreated for 30 min with either 20 mM ammonium chloride (B to D and K), 40 μM chloroquine (H and L), or 250 nM bafilomycin A (F and G) prior to incubation with *F. tularensis* Schu S4 (A to D), RCI (E to H), or LVS (I to L) at an MOI of 15:1 (ratio of bacteria to macrophages) in the presence or absence of the same inhibitors for 90 min at 37°C. Monolayers were washed to remove extracellular bacteria, incubated for 7 h in the presence of the same inhibitors, and then fixed and prepared for transmission electron microscopy. Examples of clearly defined membrane bilayers and intraphagosomal bacteria at 7 h postinfection in the absence of inhibitors of acidification are indicated by arrowheads in panel A for *F. tularensis* Schu S4 and by arrows in panel I for LVS. (Bacteria are indicated by asterisks in all panels.) At this time, most phagosomal membranes (when present) appear as typical thin membrane bilayers (arrowheads in panel A and arrows in panel I). However, dense fibrillar coats were also observed frequently (arrowheads in panel E). We found that inhibitors of acidification did not prevent *F. tularensis* from escaping into the cytoplasm at 7 h postinfection for any of the three strains. Examples of *F. tularensis* that escaped into the cytoplasm despite the presence of inhibitors of acidification are shown for Schu S4 (B to D), RCI (F to H), and LVS (K and L). The unique densely staining fibrillar coats also formed despite the presence of acidification inhibitors (arrowheads in panel C). Size bars = 0.5 μm. (M to O) Quantitation of the impact of treatment of MDM with acidification inhibitors on phagosomal escape 7 h postinfection for *F. tularensis* Schu S4 (M), RCI (N), and LVS (O). Except where noted, the culture medium was supplemented with ferric ammonium citrate (FAC) to reverse the iron sequestration known to accompany inhibition of acidification. In the absence of inhibitors of acidification, approximately 50% of the fully virulent *F. tularensis* Schu S4 (M) and RCI (N) bacteria and approximately 35% of the attenuated *F. tularensis* LVS bacteria (O) were observed to be free in the host cell cytoplasm. For all three strains, treatment of macrophage monolayers with inhibitors of acidification did not prevent escape of the bacteria into the host cell cytoplasm. Even in the absence of supplemental ferric ammonium citrate, the Schu S4 strain continued to escape into the cytoplasm. The bars and error bars indicate the means and standard errors for assessments of at least 40 cells on each of three electron microscopy grids.

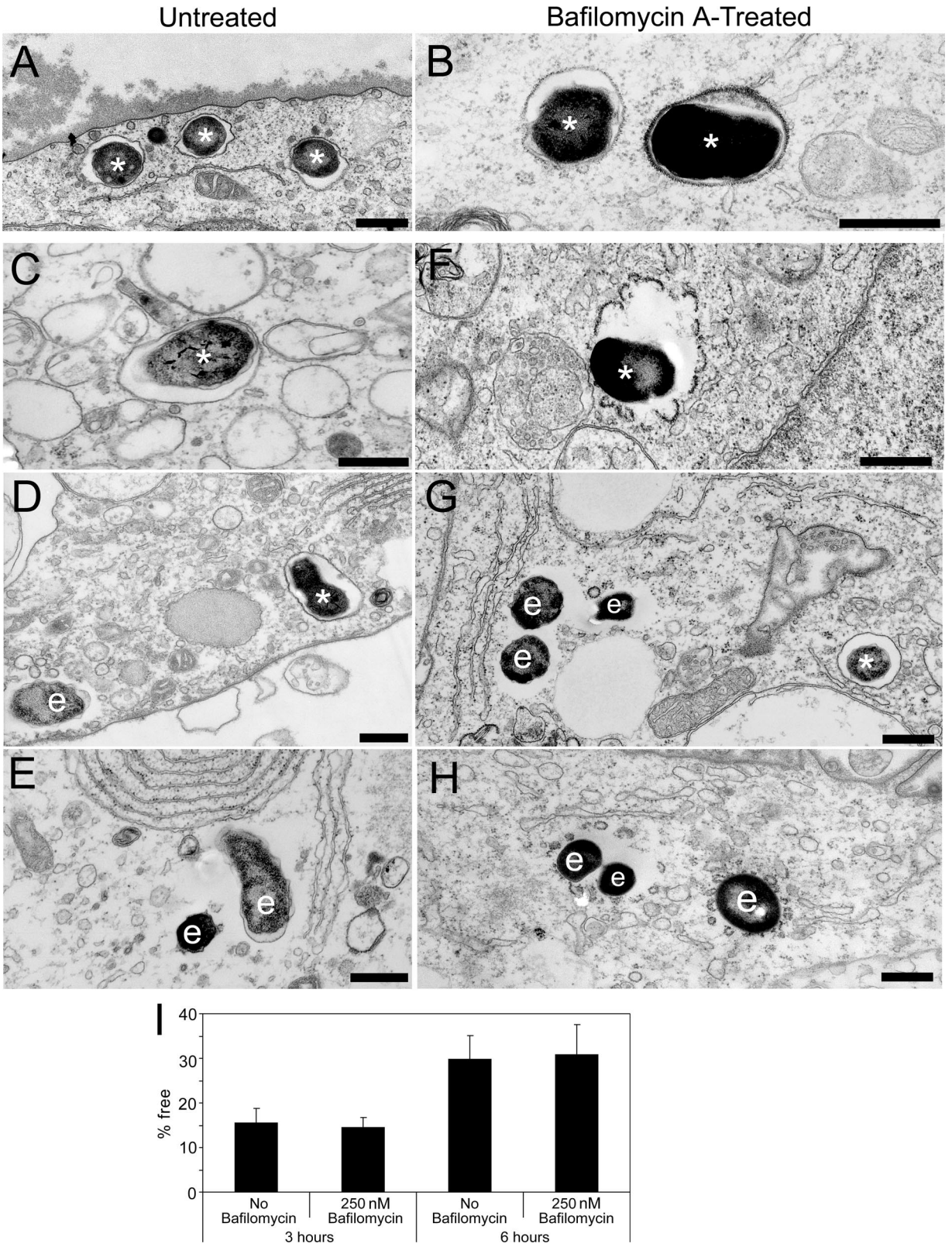

FIG. 5. Ultrastructural analysis of the impact of bafilomycin A on *F. tularensis* LVS phagosome escape in human MDM. Monolayers of human MDM were left untreated (A and C to E) or were pretreated for 30 min with bafilomycin A (B and F to H) prior to infection with *F. tularensis* LVS in the presence or absence 250 nM bafilomycin A and 0.1 mg/ml ferric ammonium citrate. Infection was continued for 3 h (A and B) or 6 h (C to H) under the same conditions, and then the monolayers were fixed and prepared for transmission electron microscopy. *F. tularensis* LVS bacteria residing within vacuoles with easily discernible membrane bilayers at 3 h are indicated by asterisks. The LVS bacterium indicated by an asterisk in panel F resided within a phagosome with a fibrillar coat that appears to be disintegrating. Bacteria that escaped into the cytoplasm are indicated by "e." Size bars = 0.5 μm. (I) Quantitation of escape into the cytoplasm. Approximately 15% and 35% of LVS bacteria escaped into the cytoplasm by 3 h and 6 h, respectively, regardless of bafilomycin A treatment. The bars and error bars indicate the means and standard errors for assessments of at least 40 cells on each of three electron microscopy grids.

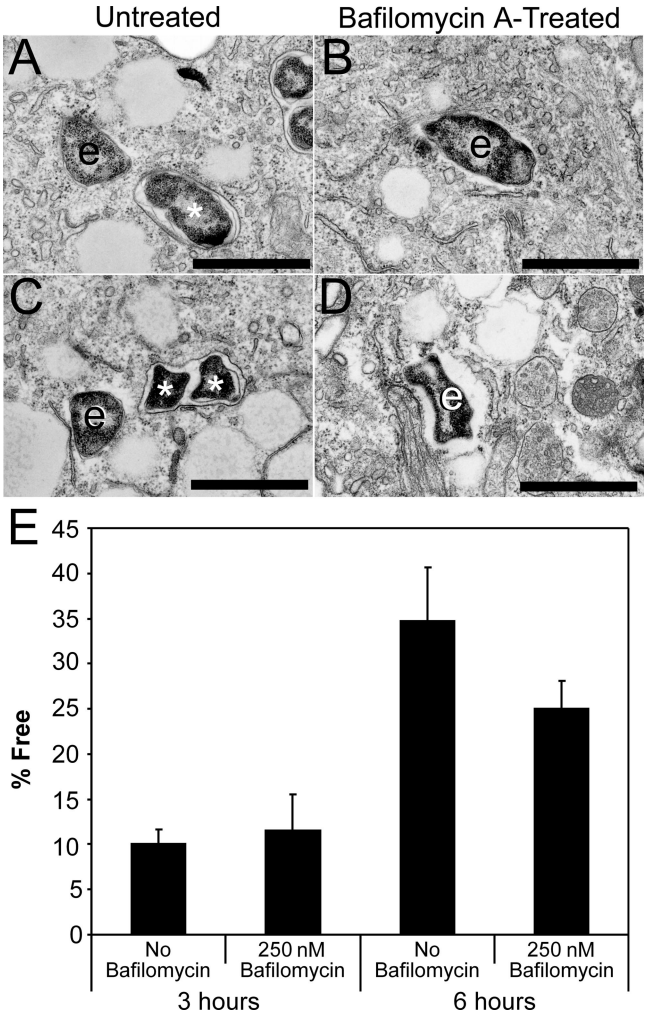

FIG. 6. Ultrastructural analysis of the impact of bafilomycin A on *F. novicida* phagosome escape in human MDM. Monolayers of human MDM were left untreated (A and C) or were pretreated for 30 min with bafilomycin A (B and D) prior to infection with *F. tularensis* subsp. *novicida* in the presence or absence 250 nM bafilomycin A and 0.1 mg/ml ferric ammonium citrate. Infection was continued for 3 h (A and B) or 6 h (C and D) under the same conditions, and then the monolayers were fixed and prepared for transmission electron microscopy. *F. tularensis* subsp. *novicida* bacteria residing within vacuoles with easily discernible membrane bilayers at 3 h (A) and 6 h (C) are indicated by asterisks. *F. tularensis* subsp. *novicida* bacteria that escaped into the cytoplasm by 3 h (A and B) or 6 h (C and D) are indicated by "e." Size bars = 0.5 μm. (E) Quantitation of escape into the cytoplasm. Approximately 10% and 30% of *F. tularensis* subsp. *novicida* bacteria escaped into the cytoplasm by 3 h and 6 h, respectively, with or without bafilomycin A treatment. The bars and error bars indicate the means and standard errors for assessments of at least 40 cells on each of three electron microscopy grids.

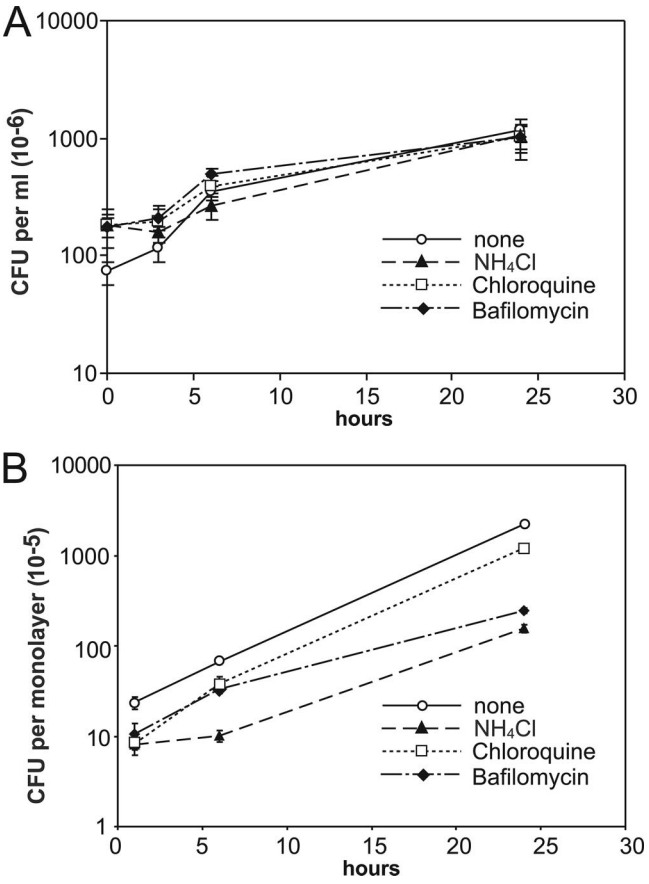

FIG. 7. Impact of NH_4Cl, chloroquine, and bafilomycin A on growth of *F. tularensis* LVS in chemically defined liquid culture (A) and in macrophage-like THP-1 cells (B). (A) *F. tularensis* LVS was grown at 37°C in chemically defined liquid culture medium (5) in the presence or absence of 20 mM ammonium chloride, 40 μM chloroquine, or 250 nM bafilomycin A, and the number of CFU was evaluated over time. (B) PMA-differentiated THP-1 cells (1.2×10^6 cells) were infected with LVS at an MOI of 2:1 by centrifugation as described in Materials and Methods, washed, and incubated at 37°C for 1 h, 5 h, or 24 h prior to enumeration of CFU in the monolayers. Monolayers either were left untreated or were treated for 30 min with ammonium chloride (20 mM), chloroquine (40 μM), or bafilomycin A (250 nM) in the presence of supplemental iron (0.1 mg/ml ferric ammonium citrate [17.5 μg/ml of iron]) prior to infection and then maintained in Dulbecco modified Eagle culture medium with the same inhibitor concentrations during subsequent incubations. The values are means and standard deviations of duplicate determinations. The experiment was performed twice with similar results.

likely because a smaller percentage of the bacteria had escaped and replicated in the cytoplasm at 5 h than at 11 h (11). In macrophages treated with bafilomycin A (250 nM) and infected with LVS-sCyaA′, we observed an approximately 50% reduction in the level of cAMP generated per monolayer and per bacterial CFU compared with the results for untreated macrophages. However, despite bafilomycin A treatment, we continued to observe much higher levels of cAMP in macrophages infected with LVS-sCyaA′ (producing the secreted form of adenylate cyclase) than in macrophages infected with LVS-CyaA′ (producing the nonsecreted form of adenylate cyclase) or with the *iglC*-null LVS-sCyaA′ (which is unable to escape from its phagosome [Fig. 9]), indicating that bacteria continue to escape despite prevention of acidification. The reduction in cAMP generation in the bafilomycin-treated, LVS-sCyaA′-infected monolayers compared to that measured in the untreated monolayers could reflect impaired or delayed phagosomal permeabilization. However, if acidification were essential for *F. tularensis* phagosome permeabilization, then the bafilomycin A treatment of the macrophages should have prevented cAMP levels in the LVS-sCyaA′-infected monolay-

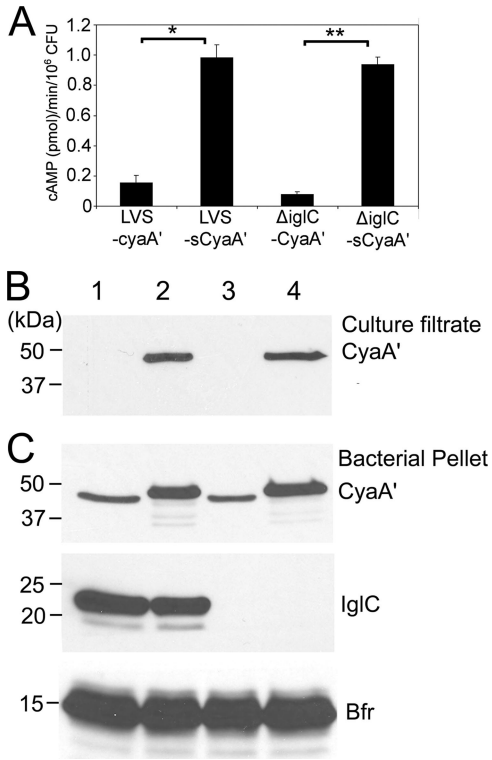

FIG. 8. Secretion of CyaA′ by recombinant strains of *F. tularensis*. LVS and *iglC*-deficient LVS (Δ*iglC*) bearing pFNLTP plasmids encoding either sCyaA′ (the leader sequence and the first 20 amino acid residues of the mature KatG fused to CyaA′) (resulting in strains designated LVS-sCyaA′ and ΔiglC-sCyaA′, respectively) or CyaA′ (without fusion with *katG*) (resulting in strains designated LVS-CyaA′ and ΔiglC-CyaA′, respectively) were grown on chocolate agar plates with 10 μg/ml kanamycin at 37°C in the presence of 5% CO_2, inoculated into chemically defined liquid culture medium (5) at an optical density of 0.1, and grown at 37°C and 200 rpm for 11 h. The cultures grew to nearly identical optical densities at 540 nm (0.371, 0.361, 0.42, and 0.436 for ΔiglC-CyaA′, ΔiglC-sCyaA′, LVS-CyaA′, and LVS-sCyaA′, respectively). Bacteria were removed by centrifugation and by filtration through 0.45- and 0.2-μm filters, and each culture supernatant was concentrated with Centricon (5,000-molecular-weight-cutoff) filter concentrators. Aliquots of culture filtrates either were assayed for adenylate cyclase activity by an assay that measures conversion of [^{32}P]ATP to [^{32}P]cAMP (A) or were analyzed by Western immunoblotting with anti-adenylate cyclase monoclonal antibody (B). The error bars indicate standard deviations of duplicates; asterisks indicate statistically significant differences (*, $P < 0.01$; **, $P < 0.001$; two-tailed unpaired Student's *t* tests). Bacteria were sonicated, and aliquots of the sonicated bacteria were also analyzed by Western immunoblotting (C) with mouse anti-adenylate cyclase monoclonal antibody, rabbit antibody to IglC, or rabbit anti-bacterioferritin (Bfr) antibody. The adenylate cyclase enzymatic activity (A) was much greater in the culture filtrates of LVS-sCyaA′ and ΔiglC-sCyaA′ than in the culture filtrates of LVS-CyaA′ and ΔiglC-CyaA′. Western immunoblotting of the culture filtrates (B) revealed a strong 48-kDa band corresponding to secreted CyaA′ in lanes 2 and 4, corresponding to LVS-sCyaA′ and ΔiglC-sCyaA′, respectively. CyaA′ was absent in lanes 1 and 3, corresponding to LVS-CyaA′ and ΔiglC-CyaA′, respectively. Western immunoblotting of the sonicated bacterial pellets (C) revealed comparable levels of bacterioferritin (15 kDa) (bottom blot) in all lanes. CyaA′ was present in all lanes (middle blot); because it has the first 20 amino acids of the mature KatG, the CyaA′ from LVS-sCyaA′ and ΔiglC-sCyaA′ (lanes 2 and 4, respectively) has a slightly higher molecular weight as determined by sodium dodecyl sulfate-polyacrylamide gel electrophoresis than the CyaA′ from LVS-CyaA′ and ΔiglC-CyaA′ (lanes 1 and 3, respectively). IglC immunoreactivity was detected in the sonicated bacterial pellets of LVS-CyaA′ (lane 1) and LVS-sCyaA′ (lane 2) but not in the lanes loaded with sonicated bacterial pellets of ΔiglC-CyaA′ (lane 3) or ΔiglC-sCyaA′ (lane 4). The experiment was conducted twice with similar results.

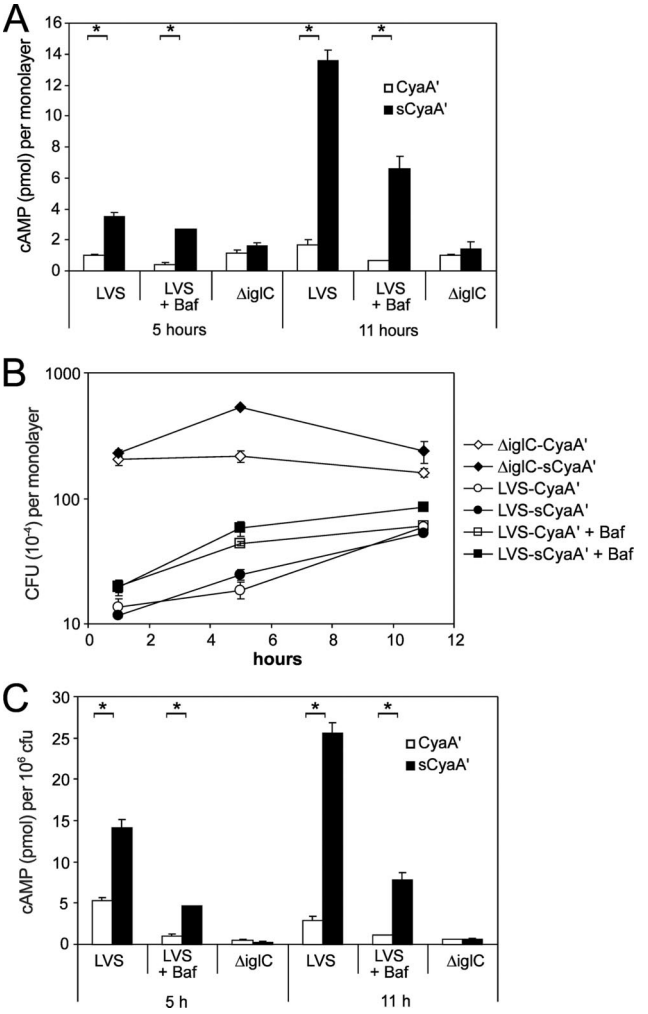

FIG. 9. Use of a CyaA′ reporter system to assess the impact of bafilomycin A on *F. tularensis* phagosome permeabilization. THP-1 cells, either untreated or treated with 250 nM bafilomycin A, were infected with LVS or an LVS IglC-deficient mutant bearing a plasmid encoding either a secreted form of CyaA′ (LVS-sCyaA′ and ΔiglC-sCyaA′, respectively) or, as a negative control, a nonsecreted form of CyaA′ (LVS-CyaA′ and ΔiglC-CyaA′, respectively). Untreated macrophages were infected with LVS-sCyaA′ or LVS-CyaA′ at an MOI of 2:1 (ratio of bacteria to macrophages). Because bafilomycin A pretreatment of macrophages decreases the uptake of *F. tularensis* (Fig. 7B), the macrophages pretreated with bafilomycin A were infected using a twofold-higher MOI (4:1). Because the ΔiglC-LVS mutants are unable to replicate inside macrophages, a 10-fold-higher MOI (20:1) was used to infect macrophages with the Δ*iglC* mutants. Levels of cAMP were measured at 5 and 11 h postinfection (A), and the numbers of bacterial CFU were determined at 1, 5, and 11 h postinfection (B). Because the amount of cAMP generated is influenced by the numbers of intracytoplasmic bacteria secreting recombinant CyaA′, the ratio of the amount of cAMP generated to the number of bacteria in each condition is shown for 5 and 11 h postinfection (C). At 5 and 11 h postinfection, in untreated THP-1 cells and in bafilomycin A-treated cells, the level of cAMP generated is markedly greater in the LVS-sCyaA′-infected THP-1 cells than in the LVS-CyaA′-infected THP-1 cells, consistent with escape of the bacteria into the cytoplasm in the presence or absence of bafilomycin A. The error bars indicate standard deviations for duplicates; the asterisks indicate statistically significant differences (*, $P \leq 0.01$, two-tailed unpaired Student's *t* tests). The levels of cAMP are not significantly greater in macrophages infected with ΔiglC-sCyaA′ than in macrophages infected with ΔiglC-CyaA′, consistent with the inability of the ΔiglC-LVS mutant to escape into the cytoplasm. The experiment was conducted three times with similar results.

ers from being greater than the levels in LVS-CyaA′- or *iglC*-null LVS-sCyaA′-infected monolayers. Moreover, it should be noted that whereas the *iglC*-null LVS-sCyaA′ bacteria are unable to grow in the macrophage monolayers (Fig. 9B), consistent with their inability to escape from the phagosome, both LVS (Fig. 7B) and LVS-sCyaA′ (Fig. 9B) do grow within macrophages despite treatment of the macrophages with bafilomycin A. Again, if bafilomycin A prevented phagosome permeabilization, then growth of the bacteria within the macrophages would not have been expected.

Live *F. tularensis* shows reduced colocalization with LysoTracker red. Although we observed that acidification of the phagosome is not required for phagosome escape, this did not rule out the possibility that the phagosome might be transiently acidified prior to escape. We have previously measured slight acidification of the phagosome to a pH of 6.7 at 3 h postinfection and found that live LVS, unlike killed LVS, does not colocalize with LysoTracker red, a marker of acidified compartments (11). To assess more thoroughly the possibility that the *F. tularensis* phagosome might be significantly acidified at earlier times, we examined LysoTracker red colocalization with live and dead *F. tularensis* at different times from 15 min to 6 h postinfection (Fig. 10). We found that whereas 70 to 90% of killed *F. tularensis* bacteria colocalize with LysoTracker red at all time points, only 20 to 30% of live LVS bacteria colocalize with LysoTracker red at these time points (Fig. 10), consistent with the hypothesis that killed LVS, but not live, LVS resides in acidified phagolysosomes. While some of the live LVS bacteria did colocalize with LysoTracker red (Fig. 10A to C and G to I), the intensity of fluorescent staining was considerably less than that for killed LVS (Fig. 10D to F and J to L). Latex beads that resided in the perimeter of the macrophages colocalized with LysoTracker red with kinetics similar to those of killed LVS (Fig. 10M). In the case of LVS, we identified noninternalized bacteria by staining the nonpermeabilized monolayers with a blue fluorescent antibody (AMCA) and found that at all of the time points examined, less than 1% of the LVS bacteria were outside the macrophages (i.e., accessible to the blue fluorescent antibody). For the latex beads, we were unable to determine the percentages of ingested beads and adherent beads; instead, we scored the beads that resided in the perimeter of the macrophages. Neither latex beads nor bacteria that were outside the borders of the macrophages colocalized with LysoTracker red. We also examined LysoTracker red staining of live macrophages (without fixation) and observed relative exclusion of LysoTracker red from live LVS but strong colocalization of LysoTracker red with latex beads (Fig. 11), indicating that the absence of colocalization of LysoTracker red staining with live LVS is not attributable to loss of the stain during fixation. Imaging of LysoTracker red colocalization with paraformaldehyde-killed LVS-GFP is technically complicated by the decrease in the fluorescence of GFP at acidic pH. (This is not a problem in paraformaldehyde-fixed monolayers, because the specimen is mounted in a neutral-pH medium and the pH is neutral throughout the specimen during imaging.)

Live *F. tularensis* shows reduced colocalization with the vATPase. Several mechanisms could allow a pathogen to resist acidification of its compartment. While decreased recruitment of the vATPase is one mechanism (as proposed for *Mycobacterium avium* and *Mycobacterium tuberculosis* [36, 40]), other mechanisms are also conceivable. For example, reduced acidification would result from (i) permeabilization of the phagosome that allows equilibration of the phagosomal pH with the cytosolic pH, (ii) persistence of the Na^+/K^+-ATPase (which generates a positive membrane potential within the vacuole, thereby opposing H^+ transport by the vATPase into the vacuole [14]), or (iii) generation of alkalinizing ammonia by the bacterium, as has been shown for *Helicobacter pylori* (35). Because we have observed that at all time points an *F. tularensis* phagosome has much less staining for lysosome-associated membrane glycoproteins than phagosomes containing either latex beads or killed *F. tularensis* have and because we have observed that live *F. tularensis* phagosomes do not acquire cathepsin D or Texas Red dextran (11), we considered the possibility that the recruitment of the vATPase, which accompanies phagosomal maturation and acidification, might also be reduced. To test this hypothesis, we stained infected macrophages by immunofluorescence for vATPase subunit 6A. Whereas killed *F. tularensis* LVS and latex beads colocalized intensely with the vATPase (Fig. 12), live *F. tularensis* LVS showed markedly reduced colocalization (Fig. 12). The reduced level of colocalization is not attributable to phagosomal escape, as the immunofluorescence observations included time points from 15 min to 3 h postinfection, times at which we observed the majority of the *F. tularensis* bacteria to be within easily discernible membrane bilayers.

DISCUSSION

Pathogens that enter the endosomal-lysosomal pathway must either adapt to the more acidic environment of this pathway or prevent acidification of their compartment. While the *F. tularensis* vacuole exhibits a limited interaction with the endocytic pathway, we have found that it fails to fuse with lysosomes, and it is only minimally acidified (pH 6.7). The resistance to acidification and limited acquisition of lysosomal markers could be a result of permeabilization of the phagosomal membrane. Thus, it has been unclear whether the resistance to acidification and altered membrane trafficking reflect a primary event or whether they instead are consequence of phagosome permeabilization that follows, or even requires, a brief period of phagosome acidification. We have demonstrated that prevention of acidification, by use of either the proton pump inhibitor bafilomycin A or lysosomotropic agents, does not prevent *F. tularensis* from disrupting its phagosomal membrane. These results are consistent with our fluorescence and immunofluorescence observations that the *F. tularensis* phagosome shows only limited colocalization with the live cell acidification stain LysoTracker red and that it acquires only limited amounts of the vATPase during the first 3 h postinfection. These data suggest that permeabilization of the *F. tularensis* phagosome follows rather than precedes the alteration of the *F. tularensis* membrane trafficking pathway. These findings will help guide further studies of the pathogenic mechanisms underlying the capacity of *F. tularensis* to disrupt its phagosome and escape into the host cytoplasm.

Our results differ from those of Santic et al. (30), who have reported that 90% of *F. tularensis* subsp. *novicida* vacuoles in human MDM acquire the vATPase and are acidified (LysoTracker red positive) at 15 to 30 min postinfection and that the level of colocalization declines to 50% by 60 min postinfection.

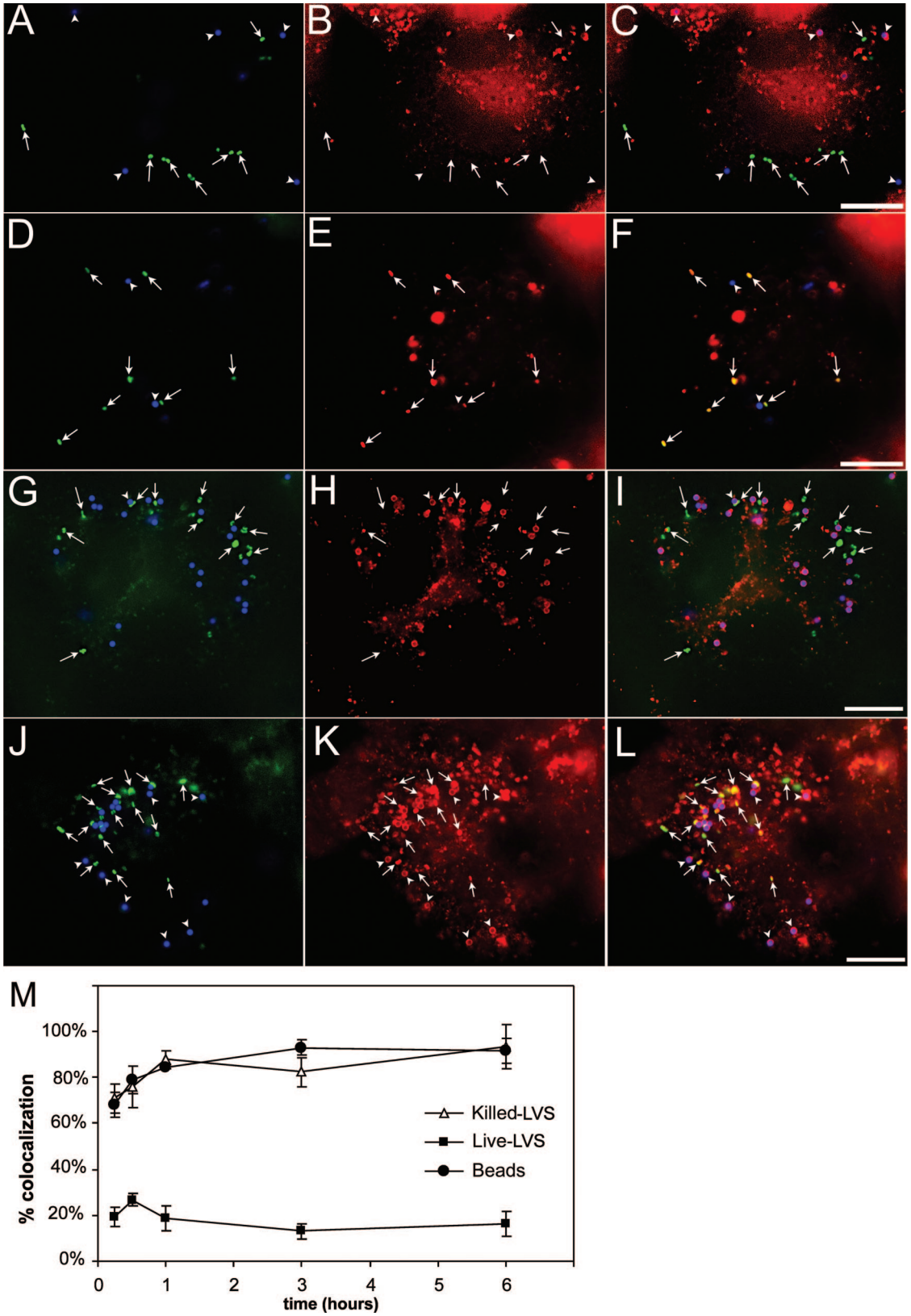

FIG. 10. Acidification of intracellular compartments in LVS-GFP-infected THP-1 macrophages assessed by LysoTracker red fluorescence. Uptake of live (A to C and G to I) or killed (D to F and J to L) LVS-GFP (green) and fluorescent blue latex beads by PMA-differentiated THP-1 cells was synchronized by centrifuging the bacteria and beads onto monolayers at 4°C. The monolayers were warmed to 37°C for 20 min, washed, incubated for an additional 30 min (A to F) or 60 min (G to L), and then fixed for evaluation by fluorescence microscopy. LysoTracker red was

While these results might be attributable to the fact that different subspecies of *Francisella* (*F. tularensis* subsp. *novicida* and *F. tularensis* subsp. *tularensis*) were studied, there are also important technical differences between the studies, and it is possible that the differences in observations may reflect differences in antibody staining conditions and in image acquisition. It is critical that fluorescence images of vATPase and LysoTracker red exhibit a vesicular-phagosomal pattern of fluorescent staining rather than diffuse fluorescence. In contrast to Santic et al. (30), we used fluorescent latex beads and killed *F. tularensis* as positive controls in our vATPase and LysoTracker red studies to establish staining conditions and camera settings that provided discrete fluorescence staining of the positive control particles without resulting in diffuse pools of fluorescence in the macrophages under examination. Using latex beads as internal positive controls, we observed relatively low levels of LysoTracker red and vATPase staining of the live *F. tularensis* LVS phagosomes but intense staining of the killed LVS phagosomes.

Our results also differ from those of Chong et al. (7), who report that 80% of *F. tularensis* Schu S4 phagosomes are acidified at 15 to 30 min postinfection. However, Chong et al. used a higher concentration of LysoTracker red than we used (0.5 μM versus 0.1 μM) and did not include latex beads as an internal control to allow comparison between different conditions. By using a much higher concentration of LysoTracker red, Chong et al. may have detected relatively mild degrees of acidification (e.g., pH 6 to 6.5), such as the acidification which is present in early endosomes. By using latex beads as an internal control, we were able to compare relative degrees of acidification between conditions, and we found that whereas phagosomes containing killed *F. tularensis* stain much more strongly for LysoTracker red than those containing latex beads (Fig. 10), phagosomes containing live *F. tularensis* acquire much less LysoTracker red than the latex bead-containing phagosomes acquire (Fig. 10 and 11), thus demonstrating that the phagosomes containing live *F. tularensis* exhibit relative resistance to acidification.

We do observe that approximately 25% of *F. tularensis* LVS bacteria do colocalize with the vATPase and with LysoTracker red at 30 min postinfection, and we cannot rule out the possibility that there is transient acidification of the *F. tularensis* phagosome. However, even transient acidification of the vacuole is not required for the bacteria to escape or to multiply within the phagosome, since continuous bafilomycin A treatment does not prevent these things from occurring. It is possible that the small subpopulation of LVS colocalizing with LysoTracker red represents bacteria that were killed or metabolically injured upon entry into the macrophage. The size of this population may subsequently decrease with time as the bacteria in the phagolysosomes are degraded (with inactivation of GFP fluorescence and loss of bacterial morphological integrity).

Whereas Santic et al. (30) report that bafilomycin blocks phagosomal escape by *F. tularensis* subsp. *novicida*, we have consistently observed that *F. tularensis* LVS, RCI, and Schu S4 disrupt their phagosomal membranes despite treatment with bafilomycin and the lysosomotropic bases ammonium chloride (LVS, RCI, and Schu S4) and chloroquine (LVS and RCI). Because we have also found that bafilomycin A treatment of macrophages does not prevent phagosomal escape of *F. tularensis* subsp. *novicida*, it is likely that methodological issues (rather than use of different *Francisella* subspecies) are the basis of the different observations. Santic et al. measured phagosomal disruption by a cytosol loading technique that involves mechanical disruption of the macrophages to allow replacement of macrophage cytosol with ambient medium containing an antibody to *F. tularensis* subsp. *novicida.* This procedure may cause changes in the osmotic, protein, and electrolyte composition within the macrophage, possibly influencing the fate of the bacterial compartment. In contrast, we have primarily used transmission electron microscopy to determine the time course of phagosomal escape by *F. tularensis* LVS, RCI, and Schu S4 and to demonstrate that inhibitors of acidification do not block this escape. By using transmission electron microscopy, we are able to verify the ultrastructural morphological integrity and health of the macrophages being examined and scored for phagosomal integrity (bacteria within macrophages that are necrotic or that have poor morphological integrity are not scored). Moreover, we have confirmed the capacity of *F. tularensis* to escape despite the presence of bafilomycin A by using an adenylate cyclase reporter system.

Chong et al. observed that prevention of acidification with proton pump inhibitors caused a delay in the otherwise rapid escape of *F. tularensis* from its phagosome in mouse macrophages (7). The assay of Chong et al. relies on differential antibody staining and the assumption that digitonin is able to permeabilize the plasma membrane without permeabilizing the *F. tularensis* phagosomal membrane. It is possible that their assay detects the presence of pores or small breaks in the phagosomal membrane that exist prior to full ultrastructural disruption of the membrane, thereby accounting for the more rapid kinetics and somewhat different observations. However,

added 15 min prior to fixation. Blue fluorescence (latex beads) (arrowheads) and green fluorescence (LVS-GFP) (arrows) are shown in panels A, D, G, and J; LysoTracker red fluorescence is shown in panels B, E, H, and K; and merged fluorescence is shown in panels C, F, I, and L. Whereas the majority of fluorescent blue latex beads (arrowheads in panels A, D, G, and J) and killed LVS-GFP (arrows in panels D and J) colocalize strongly with LysoTracker red (B, E, H, and K), the majority of live LVS (arrows in panels A and G) show little or no colocalization with LysoTracker red (arrows in panels B and E). Extracellular bacteria in these experiments were identified by staining the nonpermeabilized monolayers with rabbit anti-*F. tularensis* lipopolysaccharide and an AMCA-conjugated antibody and represented less than 1% of the total bacteria observed. Size bars = 10 μm. (M) Quantification and time course of LysoTracker red colocalization with live and formalin-killed LVS-GFP and latex beads. Uptake of live or killed LVS-GFP and latex beads by PMA-differentiated THP-1 cells was synchronized, and the colocalization of the bacteria with LysoTracker red was determined at different times after uptake as described above. Whereas killed LVS-GFP and latex beads show a high level of colocalization with LysoTracker red at all time points from 15 min to 6 h after uptake, live LVS-GFP bacteria show only 15 to 25% colocalization over the same time period. The symbols and error bars indicate the means and standard deviations of duplicate determinations for at least 100 bacteria. The experiment was conducted twice with similar results.

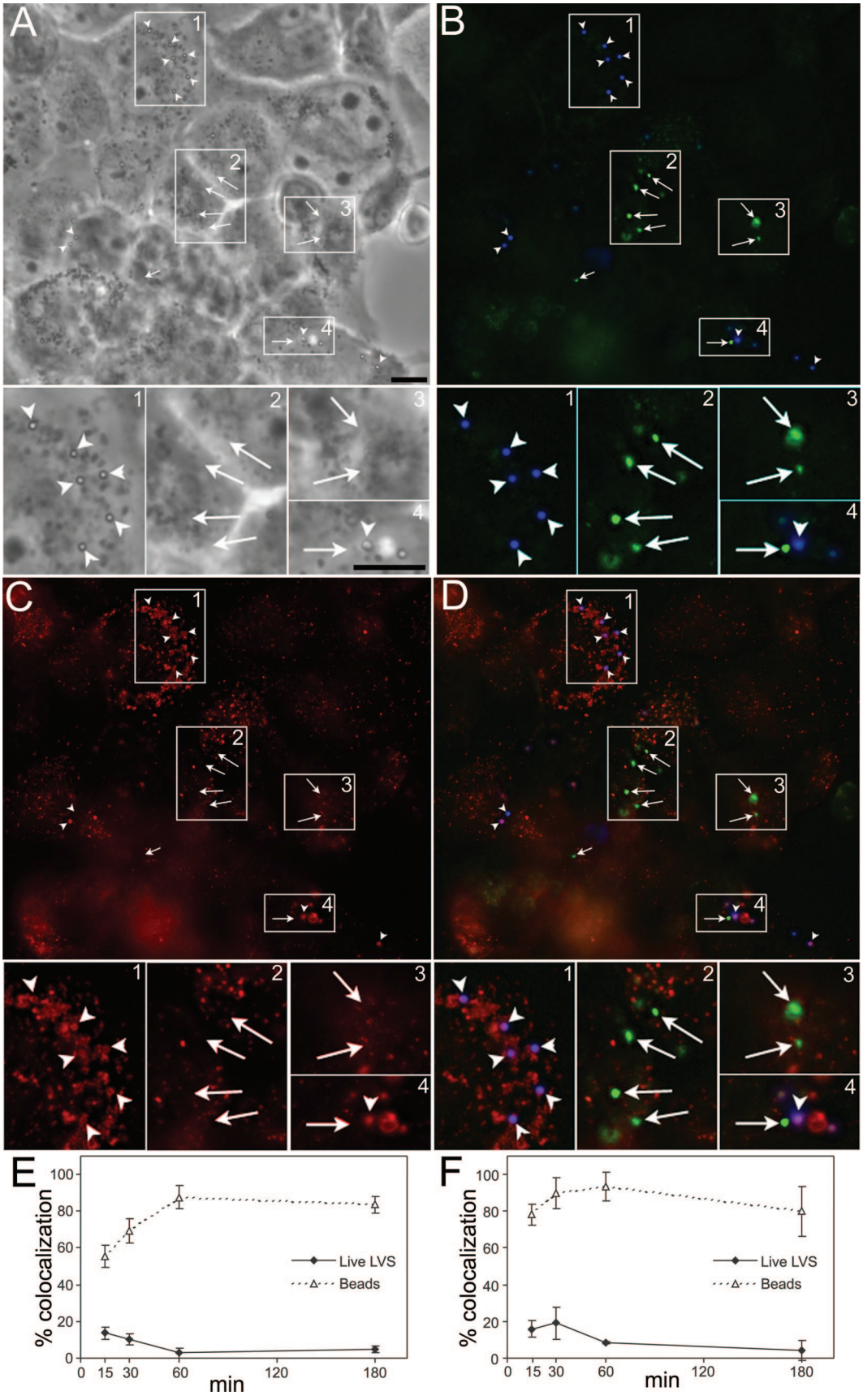
A
B
C
D
E
F
1
2
3
4
% colocalization
min
0
15
30
60
120
180
20
40
60
80
100
Live LVS
Beads

the physicochemical properties of the *F. tularensis* phagosome are not known, and it is unclear whether phagosomes that contain live *F. tularensis* are resistant to digitonin. For example, if live *F. tularensis* phagosomes were hyperosmotic relative to the host cell cytoplasm or if they had a high cholesterol content, then they may not be resistant to treatment with digitonin. It is noteworthy that, using the digitonin-based assay, Chong et al. (7) found that 30% of the *F. tularensis* subsp. *novicida iglC* mutant bacteria escape into the cytoplasm at 1 to 6 h postinfection, whereas our adenylate cyclase assay does not detect permeabilization of the phagosome by the *F. tularensis* LVS *iglC* mutant at 5 h or 11 h postinfection (Fig. 9) and Lindgren et al. (22) did not detect disruption of the phagosome by the *F. tularensis* LVS *iglC*-deficient mutant by transmission electron microscopy. While Chong et al. also employed transmission electron microscopy to assess phagosomal disruption, they did not quantify their ultrastructural observations and they considered any observed disruption of the phagosomal membrane evidence of escape. In contrast, our definition of phagosome escape requires a 50% or greater loss of membrane integrity in order to avoid misinterpretation as escape minor artifacts in sectioning, such as the knife skipping out of the plane of the section or tangential sectioning of the membrane.

In addition to the technical differences discussed above, some differences between our observations and those of Santic et al. and Chong et al. could reflect differences in the uptake pathway of the bacteria, since our macrophage infection model employs serum to promote uptake via C3 and complement receptors, whereas the methods of Santic et al. and Chong et al. do not employ serum and thus may study uptake by a nonopsonic mechanism. We use serum because we have observed that the efficiency of uptake of *F. tularensis* is greatly reduced in the absence of serum (9, 10), and it is likely that complement is present at sites of infection in vivo.

Alteration of the intracellular pH can alter the growth and multiplication of intracellular pathogens by a variety of mechanisms. Pharmacological inhibitors of acidification have a variety of effects on intracellular membrane trafficking and on the ionic and nutrient composition within a macrophage that may impact the metabolic activity of *F. tularensis*, independent of any direct impact on the pH of the *F. tularensis* vacuole (and independent of whether *F. tularensis* is even inside a vacuole). For example, Claus et al. showed that bafilomycin A and chloroquine treatment prevented delivery of proteolytic and hydrolytic enzymes to phagosomes (8), van Weert et al. showed that bafilomycin A prevented the transport of endocytosed material from late endosomes to lysosomes (37), and Presley et al. showed that bafilomycin A treatment slows both the bulk flow of membranes and the recycling of transferrin receptors (28) in CHO cells. These effects on general cellular membrane trafficking impact the catabolism of endocytosed materials and the availability of nutrients to intracellular *F. tularensis*, regardless of whether *F. tularensis* is free in the cytoplasm or inside a vacuole. Because the release of iron from iron-transferrin requires the acidification of early endosomes, agents that block endosomal-lysosomal acidification decrease the supply of iron in host cells. Thus, agents that block endosomal acidification restrict the availability of iron to intracellular pathogens and can inhibit the intracellular growth of pathogens that reside in minimally acidified phagosomes, such as *L. pneumophila* (3), which resides in a phagosome with a pH of 6.1 (19), as well as pathogens that escape into the host cell cytoplasm, such as *F. tularensis* (13). Thus, restriction of intracellular growth resulting from agents that block endosomal acidification indicates the importance of iron to intracellular growth but does not provide evidence regarding the compartment occupied by the pathogen or even the intracellular pH of the compartment occupied by the pathogen. Accordingly, the intracellular growth of both *F. tularensis* (13) and *L. pneumophila* (3) was restored by supplementation of the macrophage culture medium with iron chelation complexes, such as ferric pyrophosphate and ferric ammonium citrate, indicating that the most important effect of pH on the intracellular growth of these pathogens was mediated via iron availability. If blocking phagosome acidification actually prevented phagosomal escape of *F. tularensis* LVS (as suggested by Santic et al. [30]), then supplementation of the culture medium with ferric pyrophosphate (13) would not be expected to restore the intracellular growth.

While bafilomycin A treatment of macrophages leads to an approximately 50% reduction in cAMP generation in LVS-sCyaA′-infected macrophages, we observe relatively little impact on phagosome permeabilization by electron microscopy. This reduction in cAMP generation could be attributable to impaired or delayed formation of pores or impaired formation of small breaks in the membrane that are not apparent when

FIG. 11. Acidification of intracellular compartments in LVS-GFP-infected human macrophages assessed by LysoTracker red fluorescence of live cells. Uptake of live LVS-GFP (green) and fluorescent blue latex beads by human THP-1 cells (A to D) was synchronized as described in the legend to Fig. 10, and acidification of live macrophages was evaluated after 15 min, 30 min, 1 h, or 3 h. Acidified compartments were identified by incubation of the monolayers with LysoTracker red (0.1 μM) for 5 min at 37°C immediately prior to fluorescence microscopy. Panels A to D show THP-1 cells infected with live LVS 30 min postinfection. Phase-contrast micrographs are shown in panel A. Blue and green fluorescence channels are shown in panel B, revealing the positions of the fluorescent blue latex beads (arrowheads) and the green LVS-GFP bacteria (arrows). LysoTracker red fluorescence is shown in panel C, and merged fluorescence is shown in panel D. The numbered boxes (boxes 1 to 4) in each large micrograph indicate the areas shown at higher magnification in the corresponding small micrographs below it. Whereas almost all of the fluorescent blue latex beads (arrowheads in panel B) colocalize strongly with LysoTracker red (C), the live LVS bacteria (arrows in panel B) exhibit little or no colocalization with LysoTracker red (arrows in panel C). Size bars = 10 μm. (E and F) Quantification and time course of LysoTracker red colocalization with live LVS-GFP and latex beads in human THP-1 cells (E) and MDM (F) in nonfixed cells at 15 min to 3 h postinfection. Uptake of live LVS-GFP and latex beads was synchronized, and the colocalization of the bacteria or latex beads with LysoTracker red was determined at different times after uptake as described above. Whereas latex beads show a high level of colocalization with LysoTracker red at all time points from 15 min to 3 h after uptake, the live LVS-GFP bacteria show only 15 to 20% colocalization over the same time period. The symbols and error bars indicate means and standard deviations of duplicate determinations for at least 40 bacteria at each time point. The experiments were conducted twice with similar results.

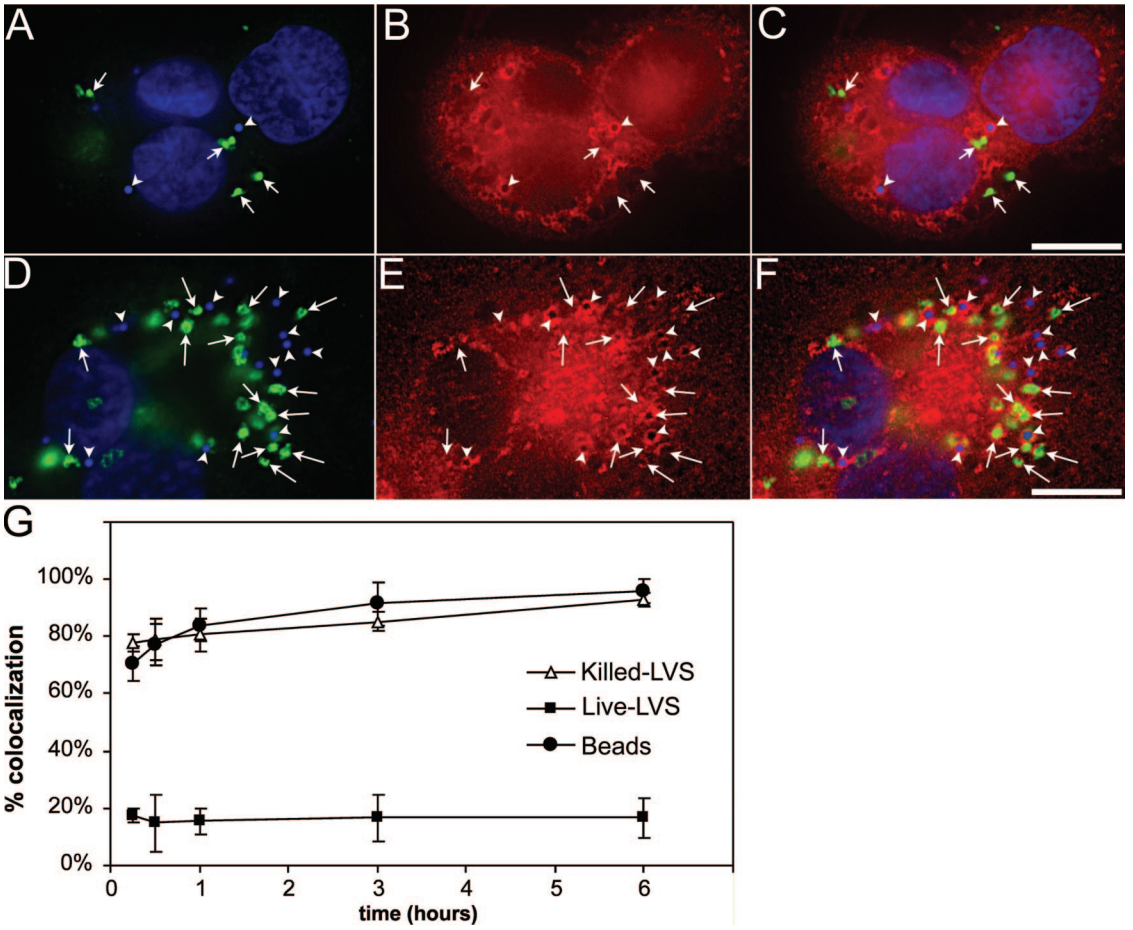

FIG. 12. Immunofluorescence assessment of colocalization of live and killed LVS-GFP with proton vATPase subunit 6A in THP-1 cells. Uptake of live (A to C) or killed (D to F) LVS-GFP and fluorescent blue latex beads by PMA-differentiated THP-1 cells was synchronized by centrifugation as described in the legend to Fig. 10. The monolayers were warmed to 37°C for 20 min, washed, incubated for an additional 60 min, and then fixed and processed for immunofluorescence microscopy. Live (A) and killed (D) *F. tularensis* bacteria are identified by green fluorescence (arrows), and latex beads are identified by blue fluorescence (arrowheads); H^+-vATPase subunit 6A was stained with a red fluorescent antibody (B and E), and merged color images are shown in panels C and F. Whereas the majority of fluorescent blue latex beads (arrowheads in panels A and D) and killed LVS-GFP (arrows in panel D) are rimmed by enhanced levels of the vATPase red immunofluorescence (B and E), the majority of live LVS bacteria (arrows in panel A) do not colocalize with the vATPase (arrows in panel B). Size bars = 10 μm. (G) Quantitation and time course of colocalization of vATPase with live and formalin-killed LVS-GFP. Uptake of live or killed LVS-GFP and latex beads by PMA-differentiated THP-1 cells was synchronized, and the colocalization of the bacteria with H^+-vATPase 6A was determined at different times after uptake as described above. Whereas killed LVS-GFP and latex beads show 70 to 90% colocalization with the vATPase at all time points from 15 min to 6 h after uptake, live LVS-GFP shows only 15 to 20% colocalization over the same time period. The symbols and error bars indicate means and standard deviations of duplicate determinations for at least 100 bacteria. The experiment was conducted twice with similar results.

electron microscopy is used. However, whereas electron microscopy allows direct assessment of phagosome permeabilization, the adenylate cyclase reporter assay is an indirect assay that may be influenced by many factors unrelated to phagosome permeabilization, such as the level of calcium, ATP, or calmodulin in the macrophage cytoplasm, the nutrients available to *F. tularensis* for metabolic activity, and the rate of adenylate cyclase protein secretion by the bacteria. Although these factors can complicate the interpretation of the results obtained using the adenylate cyclase reporter system, the fact that we observe a dramatic increase in cAMP generation in LVS-sCyaA′-infected macrophages compared to LVS-CyaA′- or *iglC*-null LVS-sCyaA′-infected macrophages despite bafilomycin A treatment indicates that acidification of the phagosome is not essential for phagosome escape.

The mechanism by which *F. tularensis* escapes from its phagosome is not clear. For other pathogens that escape from their phagosomes, porins and cytolysins have been implicated. An acidic environment is required for some but not all membrane-permeabilizing actions of porins and cytolysins. For example, the action of listeriolysin O requires an acidic pH, and the escape of *L. monocytogenes* into the host cell cytoplasm is blocked by either NH_4Cl or bafilomycin A (1). Similarly, the escape of adenoviruses from endosomes into the host cell cytoplasm requires an acidic pH-dependent change in viral proteins (23). However, the degree of acidification required for lysis varies from pathogen to pathogen. The pH required for membrane lysis of adenovirus type 7 (pH 5.5) is more acidic than the pH required for membrane lysis of adenovirus type 5 (pH 6.0) (23). On the other hand, some membrane lytic mechanisms are functional at neutral pH. Indeed,

it is noteworthy that the *Listeria*-derived cholesterol-dependent cytolysins are unique among the family of cholesterol-dependent cytolysins and that other members of this family, including pneumolysin, streptolysin O, and perfringolysin O, do not require an acidic pH for their pore-forming activity (24). Whatever molecular mechanism is involved in the escape of *F. tularensis* from its phagosome, our data indicate that it is not dependent upon an acidic pH.

ACKNOWLEDGMENTS

This work was supported by grants HL077000 and AI065359 from the National Institutes of Health.

We are grateful to Marianne Cilluffo for expert assistance with the electron microscopy and to Melissa Taylor for expert technical assistance.

REFERENCES

1. **Beauregard, K. E., K. D. Lee, R. J. Collier, and J. A. Swanson.** 1997. pH-dependent perforation of macrophage phagosomes by listeriolysin O from Listeria monocytogenes. J. Exp. Med. **186:**1159–1163.
2. **Brotcke, A., D. S. Weiss, C. C. Kim, P. Chain, S. Malfatti, E. Garcia, and D. M. Monack.** 2006. Identification of MglA-regulated genes reveals novel virulence factors in *Francisella tularensis*. Infect. Immun. **74:**6642–6655.
3. **Byrd, T. F., and M. A. Horwitz.** 1991. Chloroquine inhibits the intracellular multiplication of Legionella pneumophila by limiting the availability of iron. A potential new mechanism for the therapeutic effect of chloroquine against intracellular pathogens. J. Clin. Investig. **88:**351–357.
4. **Byrd, T. F., and M. A. Horwitz.** 1991. Lactoferrin inhibits or promotes Legionella pneumophila intracellular multiplication in nonactivated and interferon gamma-activated human monocytes depending upon its degree of iron saturation. Iron-lactoferrin and nonphysiologic iron chelates reverse monocyte activation against Legionella pneumophila. J. Clin. Investig. **88:** 1103–1112.
5. **Chamberlain, R. E.** 1965. Evaluation of a live tularemia vaccine prepared in a chemically defined medium. Appl. Microbiol. **13:**232–235.
6. **Checroun, C., T. D. Wehrly, E. R. Fischer, S. F. Hayes, and J. Celli.** 2006. Autophagy-mediated reentry of Francisella tularensis into the endocytic compartment after cytoplasmic replication. Proc. Natl. Acad. Sci. USA **103:** 14578–14583.
7. **Chong, A., T. D. Wehrly, V. Nair, E. R. Fischer, J. R. Barker, K. E. Klose, and J. Celli.** 2008. The early phagosomal stage of *Francisella tularensis* determines optimal phagosomal escape and *Francisella* pathogenicity island protein expression. Infect. Immun. **76:**5488–5499.
8. **Claus, V., A. Jahraus, T. Tjelle, T. Berg, H. Kirschke, H. Faulstich, and G. Griffiths.** 1998. Lysosomal enzyme trafficking between phagosomes, endosomes, and lysosomes in J774 macrophages. Enrichment of cathepsin H in early endosomes. J. Biol. Chem. **273:**9842–9851.
9. **Clemens, D. L., and M. A. Horwitz.** 2007. Uptake and intracellular fate of *Francisella tularensis* in human macrophages. Ann. N. Y. Acad. Sci. **1105:** 160–186.
10. **Clemens, D. L., B. Y. Lee, and M. A. Horwitz.** 2005. *Francisella tularensis* enters macrophages via a novel process involving pseudopod loops. Infect. Immun. **73:**5892–5902.
11. **Clemens, D. L., B. Y. Lee, and M. A. Horwitz.** 2004. Virulent and avirulent strains of *Francisella tularensis* prevent acidification and maturation of their phagosomes and escape into the cytoplasm in human macrophages. Infect. Immun. **72:**3204–3217.
12. **Ellis, J., P. C. F. Oyston, M. Green, and R. W. Titball.** 2002. Tularemia. Clin. Microbiol. Rev. **15:**631–646.
13. **Fortier, A. H., D. A. Leiby, R. B. Narayanan, E. Asafoadjei, R. M. Crawford, C. A. Nacy, and M. S. Meltzer.** 1995. Growth of *Francisella tularensis* LVS in macrophages: the acidic intracellular compartment provides essential iron required for growth. Infect. Immun. **63:**1478–1483.
14. **Fuchs, R., S. Schmid, and I. Mellman.** 1989. A possible role for Na^+, K^+-ATPase in regulating ATP-dependent endosome acidification. Proc. Natl. Acad. Sci. USA **86:**539–543.
15. **Geddes, K., M. Worley, G. Niemann, and F. Heffron.** 2005. Identification of new secreted effectors in *Salmonella enterica* serovar Typhimurium. Infect. Immun. **73:**6260–6271.
16. **Golovliov, I., V. Baranov, Z. Krocova, H. Kovarova, and A. Sjostedt.** 2003. An attenuated strain of the facultative intracellular bacterium *Francisella tularensis* can escape the phagosome of monocytic cells. Infect. Immun. **71:**5940–5950.
17. **Harlowe, E., and D. Lane.** 1988. Antibodies: a laboratory manual. Cold Spring Harbor Laboratory, Cold Spring Harbor, NY.
18. **Horwitz, M. A.** 1984. Phagocytosis of the Legionnaires' disease bacterium (Legionella pneumophila) occurs by a novel mechanism: engulfment within a pseudopod coil. Cell **36:**27–33.
19. **Horwitz, M. A., and F. R. Maxfield.** 1984. Legionella pneumophila inhibits acidification of its phagosome in human monocytes. J. Cell Biol. **99:**1936–1943.
20. **Lauriano, C. M., J. R. Barker, S. S. Yoon, F. E. Nano, B. P. Arulanandam, D. J. Hassett, and K. E. Klose.** 2004. MglA regulates transcription of virulence factors necessary for Francisella tularensis intraamoebae and intramacrophage survival. Proc. Natl. Acad. Sci. USA **101:**4246–4249.
21. **Lee, B. Y., M. A. Horwitz, and D. L. Clemens.** 2006. Identification, recombinant expression, immunolocalization in macrophages, and T-cell responsiveness of the major extracellular proteins of *Francisella tularensis*. Infect. Immun. **74:**4002–4013.
22. **Lindgren, H., I. Golovliov, V. Baranov, R. K. Ernst, M. Telepnev, and A. Sjostedt.** 2004. Factors affecting the escape of *Francisella tularensis* from the phagolysosome. J. Med. Microbiol. **53:**953–958.
23. **Miyazawa, N., R. G. Crystal, and P. L. Leopold.** 2001. Adenovirus serotype 7 retention in a late endosomal compartment prior to cytosol escape is modulated by fiber protein. J. Virol. **75:**1387–1400.
24. **Nomura, T., I. Kawamura, C. Kohda, H. Baba, Y. Ito, T. Kimoto, I. Watanabe, and M. Mitsuyama.** 2007. Irreversible loss of membrane-binding activity of Listeria-derived cytolysins in non-acidic conditions: a distinct difference from allied cytolysins produced by other Gram-positive bacteria. Microbiology **153:**2250–2258.
25. **Oyston, P. C., A. Sjostedt, and R. W. Titball.** 2004. Tularaemia: bioterrorism defence renews interest in Francisella tularensis. Nat. Rev. Microbiol. **2:**967–978.
26. **Pierini, L. M.** 2006. Uptake of serum-opsonized *Francisella tularensis* by macrophages can be mediated by class A scavenger receptors. Cell. Microbiol. **8:**1361–1370.
27. **Post, S. R., R. S. Ostrom, and P. A. Insel.** 2000. Biochemical methods for detection and measurement of cyclic AMP and adenylyl cyclase activity. Methods Mol. Biol. **126:**363–374.
28. **Presley, J. F., S. Mayor, T. E. McGraw, K. W. Dunn, and F. R. Maxfield.** 1997. Bafilomycin A1 treatment retards transferrin receptor recycling more than bulk membrane recycling. J. Biol. Chem. **272:**13929–13936.
29. **Salomon, Y., C. Londos, and M. Rodbell.** 1974. A highly sensitive adenylate cyclase assay. Anal. Biochem. **58:**541–548.
30. **Santic, M., R. Asare, I. Skrobonja, S. Jones, and Y. Abu Kwaik.** 2008. Acquisition of the vacuolar ATPase proton pump and phagosome acidification are essential for escape of *Francisella tularensis* into the macrophage cytosol. Infect. Immun. **76:**2671–2677.
31. **Santic, M., M. Molmeret, K. Klose, S. Jones, and Y. Kwaik.** 2005. The F. tularensis pathogenicity island protein IglC and its regulator MglA are essential for modulating phagosome biogenesis and subsequent bacterial escape into the cytoplasm. Cell. Microbiol. **7:**969–979.
32. **Saslaw, S., H. T. Eigelsbach, J. Prior, H. Wilson, and S. Carhart.** 1961. Tularemia vaccine study. I. Intracutaneous challenge. Arch. Intern. Med. **107:**121–133.
33. **Saslaw, S., H. T. Eigelsbach, J. Prior, H. Wilson, and S. Carhart.** 1961. Tularemia vaccine study. II. Respiratory challenge. Arch. Intern. Med. **107:** 702–714.
34. **Schulert, G. S., and L. A. Allen.** 2006. Differential infection of mononuclear phagocytes by Francisella tularensis: role of the macrophage mannose receptor. J. Leukoc. Biol. **80:**563–571.
35. **Schwartz, J. T., and L. A. Allen.** 2006. Role of urease in megasome formation and Helicobacter pylori survival in macrophages. J. Leukoc. Biol. **79:**1214–1225.
36. **Sturgill-Koszycki, S., P. H. Schlesinger, P. Chakraborty, P. L. Haddix, H. L. Collins, A. K. Fok, R. D. Allen, S. L. Gluck, J. Heuser, and D. G. Russell.** 1994. Lack of acidification in *Mycobacterium* phagosomes produced by exclusion of the vesicular proton-ATPase. Science **263:**678–681.
37. **van Weert, A. W., K. W. Dunn, H. J. Gueze, F. R. Maxfield, and W. Stoorvogel.** 1995. Transport from late endosomes to lysosomes, but not sorting of integral membrane proteins in endosomes, depends on the vacuolar proton pump. J. Cell Biol. **130:**821–834.
38. **Whipp, M. J., J. M. Davis, G. Lum, J. de Boer, Y. Zhou, S. W. Bearden, J. M. Petersen, M. C. Chu, and G. Hogg.** 2003. Characterization of a novicida-like subspecies of Francisella tularensis isolated in Australia. J. Med. Microbiol. **52:**839–842.
39. **Wolff, J., G. H. Cook, A. R. Goldhammer, and S. A. Berkowitz.** 1980. Calmodulin activates prokaryotic adenylate cyclase. Proc. Natl. Acad. Sci. USA **77:**3841–3844.
40. **Xu, S., A. Cooper, S. Sturgill-Koszycki, T. van Heyningen, D. Chatterjee, I. Orme, P. Allen, and D. G. Russell.** 1994. Intracellular trafficking in *Mycobacterium tuberculosis* and *Mycobacterium avium*-infected macrophages. J. Immunol. **153:**2568–2578.

Editor: W. A. Petri, Jr.